

Article

Importance of the Spatial Distribution of Rare Earth Elements in the Bottom Sediments of Reservoirs as a Potential Proxy for Tracing Sediments Sources. A Case Study in the Dominican Republic

Rita Fonseca ^{1,2,*}, Joana Fonseca Araújo ¹  and Catarina Gomes Pinho ¹ 

¹ AmbiTerra Laboratory, Earth Science Institute (ESI), University of Évora, 7005-345 Évora, Portugal; jfaraujo@uevora.pt (J.F.A.); c_pinho@uevora.pt (C.G.P.)

² Department of Geosciences, School of Science and Technology, University of Évora, 7002-554 Évora, Portugal

* Correspondence: rfonseca@uevora.pt; Tel.: +351-266-745-301

Abstract: The geochemical composition of rare earth elements (REE) in the bottom sediments of two Dominican reservoirs and in soils from their catchments was studied to identify possible sources of the deposited materials. Knowledge of the origin of the sediments will serve to control the excessive rates of erosion and sedimentation that occur annually due to periodic extreme climatic events that promote excessive silting of the lakes, followed by loss of storage capacity and degradation of water quality. The REE contents of sediments and soils were normalized to the North American Shale Composite (NASC) and the ratio of light/heavy rare earths (LREE/HREE ratio), Ce and Eu anomalies, and some fractionation parameters were determined. The REE patterns are more homogeneous in the sediments, indicating uniform sedimentation in both deposits. The sediment data reflect depletion of REE from the sources, enrichment of light REE (LREE) and some middle REE (MREE), and positive Eu and Ce anomalies. All data were plotted in correlation diagrams between some fractionation parameters of light–middle–heavy REE and anomalies of Ce and Eu. The similarity of the ratios between these parameters in all samples and the overlap of data from soils and rocks on the sediment projection in the diagrams allowed a good discrimination of the main sources of the materials.

Keywords: dam reservoirs; drainage basins; extreme climatic events; geochemical analysis; rare earth elements; sediments provenance



Citation: Fonseca, R.; Araújo, J.F.; Pinho, C.G. Importance of the Spatial Distribution of Rare Earth Elements in the Bottom Sediments of Reservoirs as a Potential Proxy for Tracing Sediments Sources. A Case Study in the Dominican Republic. *Geosciences* **2021**, *11*, 490. <https://doi.org/10.3390/geosciences11120490>

Academic Editors:

Jesus Martinez-Frias and Luca Mao

Received: 26 October 2021

Accepted: 26 November 2021

Published: 30 November 2021

Publisher's Note: MDPI stays neutral with regard to jurisdictional claims in published maps and institutional affiliations.



Copyright: © 2021 by the authors. Licensee MDPI, Basel, Switzerland. This article is an open access article distributed under the terms and conditions of the Creative Commons Attribution (CC BY) license (<https://creativecommons.org/licenses/by/4.0/>).

1. Introduction

Sediments are often reservoirs of many substances in aquatic environments, especially in lakes fed by rivers that receive water and sediments from upstream tributaries [1,2]. Their mineralogical and geochemical “fingerprints” are mainly determined by the properties of the source rocks and the climatic conditions of the catchments [3]. The concentration of certain chemical elements can be used as a tracer to define the sources of the sediments [4–6], especially the geochemically immobile elements such as Al, Fe, Th, Ti, Sc, Co, Zr, and, above all, the rare earth elements (REE), which are transported as particulate load [7,8]. The most important contribution of the analysis of REE in clastic sediments is the analysis of their origin [9]. This coherent group of elements occurs in very small amounts in natural waters, has a short hydraulic residence time in aquatic systems, and is therefore little affected by the mixing and homogenization effects of erosion and sedimentation processes, resulting in uniform patterns of REE in sedimentary materials that reflect their content in source rocks [7,10]. This group occurs as trace elements in most rock types and is highly electropositive. Their most common oxidation state is +3, although europium and cerium are also stable in tetravalent and divalent oxidation states under certain environmental conditions [11], which depend on temperature, pressure, composition, and redox conditions [12]. They can be classified into light rare elements (LREE, including La,

Ce, Pr, Nd, Sm, and Eu) and heavy REE (HREE, including Gd, Tb, Dy, Ho, Er, Yb, and Lu). They can also be considered as the members of the medium atomic number group (MREE), which includes the elements from Sm to Ho [9].

The key role of REE in the identification of sedimentary sources is based on the assumption that they are relatively conservative [13], suffer little geochemical fractionation during weathering, transport, and deposition processes, and are highly resistant to physical and chemical mobilization. They reflect the mineralogical and geochemical signatures of the basin rocks [14,15] and indicate the geochemical evolutionary processes of the sedimentary systems [16,17]. During these processes, they are usually concentrated in the fine-grained sediments because their host minerals, such as oxides (e.g., titanite), halides, carbonates, phosphates (e.g., apatite), and silicates (e.g., zircon, epidote, garnet, clays) occur in this size range. Therefore, they are transported in rivers mainly as suspended solids, leaving behind bedload depleted in REE and rich in quartz and feldspar [14], and are preferentially concentrated in lakes where fractionation of these elements can be expected.

In lake studies, the role of REE as a source tracer for sediments must be carefully evaluated because sediment chemistry is largely controlled by physical and chemical processes that regulate the transport, deposition, and availability of their particulate or dissolved forms from soils and rocks in the basins to these lacustrine systems [18]. For example, when seasonal changes in redox conditions occur, they can have an impact on the concentrations of REE species that are most sensitive to redox conditions, such as cerium and europium [15,18–20]. The chemistry of REE in lake sediments is a product of exchanges between surface water, mineral surfaces, and pore water and is the result of a series of complex processes which, according to [18] and [21], include (1) the origin of the sediments, (2) physical and chemical processes that regulate the transport and availability of dissolved and particulate REE from source rocks and soils into lakes, and (3) the chemistry of the water from which the particles settle (water column salinity, physical mixing, groundwater discharge, seasonal anoxia conditions).

Given the drawbacks of identifying sediment sources from REE, their distribution, geochemical properties, and fractionation patterns are important tools for understanding the mechanisms by which REE accumulate in lake sediments, and thus identifying their origin or nature [13,20,22,23].

The aim of this study is to present the most comprehensive data on the study of rare earth elements in the sediments of two reservoirs in the Dominican Republic (Sabana Yegua and Tavera). Comparison of the contents, spatial distribution, and fractionation patterns of REE of the sediments with those of representative soils and rocks from their catchments was used as an initial proxy to identify sediment sources. The results obtained with these elements will be compared, in the near future, with other fingerprinting analyses involving other chemical elements. This knowledge is particularly important to better control the excessive erosion and resulting sedimentation rates that occur each year in these reservoirs and the resulting degradation of water quality, energy production, and loss of storage capacity. These problems are caused by the tropical climate, exacerbated by periods of extreme climatic events, and by the high complexity of these systems, where there are strong climate–soils–rivers–lakes interactions in the basins.

2. Characterization of the Area

The Dominican Republic has a tropical climate, enhanced by extreme hydrometeorological events that occur almost every year. This climate, in a volcanic region with pronounced slopes and fine-grained soils, favors the transport and deposition of finer particles in the reservoirs, affecting their structure and function by increasing sedimentation rates, altering the supply and processing of nutrients and organic matter, and degrading water quality.

The selected reservoirs are located near the highest mountain zone (Cordillera Central). Sabana Yegua has the largest catchment area of all the reservoirs in the Dominican Republic, with an area of 1669.80 km², while Tavera's catchment area is only 783.38 km². Both catch-

ments have identical lithology and different climatic conditions, Tavera (T) in the north with higher rainfall rates (1880 mm/year) and Sabana Yegua (SY) in the south where the climate is drier (annual rainfall rates: 1265 mm/year). Although average rainfall rates do not show significant annual variations, in the year in which this work was carried out (2017), the highest rainfall rates were observed between December and April, and the driest period was between April and July, the latter corresponding to the period in which the floodgates open and consequently the lowest level of the water column is reached. The high rainfall rates in the catchments with steep slopes (1.93% in Tavera and 4.15% in Sabana Yegua) have resulted in high sedimentation rates. Studies conducted in both catchments by [24] revealed an average sedimentation rate of (1) in Tavera: 2295 m³/km²/year (during the period 1973–1993) and (2) in Sabana Yegua: 1246 m³/km²/year (during the period 1979–2008). These rates show a heterogeneous distribution over the period in which they were calculated, depending on the occurrence of six major episodes of extreme climatic events.

Tavera has only one tributary (the Yaque del Norte River), while Sabana Yegua has three (the Yaque del Sur, Grande del Medio, and Las Cuevas Rivers). Due to their location in areas with steep slopes, they are deep lakes (maximum depth at maximum storage capacity, 80 m in Tavera and 76 m in Sabana Yegua) with small surface area and medium storage volume (21 km² and 479.9 million m³ in Sabana Yegua, and 6.20 km² and 173 million m³ in Tavera). The Tavera reservoir is connected to the Bao reservoir by a 1.5 km long canal. This dam was built in a tributary of the Yaque del Norte at a later date to allow Bao to supply its water to Tavera in emergencies of water need, with hydropower generation also being a priority. The sediment survey took place only in Tavera, as the main river has the highest percentage of sediment and thus has a higher siltation rate.

The Tavera and Sabana Yegua basins are contiguous and are characterized by a wide variety of igneous rocks (from ultrabasic to intermediate composition), volcano-sedimentary rocks with island-arc origins, metamorphic rocks, and detrital and carbonate sedimentary rocks. The main differences between the two basins are that Tavera has a greater extent of tonalitic, basic, and ultrabasic igneous rocks, while Sabana Yegua has a greater influence of volcanic sedimentary, carbonate, and detrital rocks as sources (Figure 1).

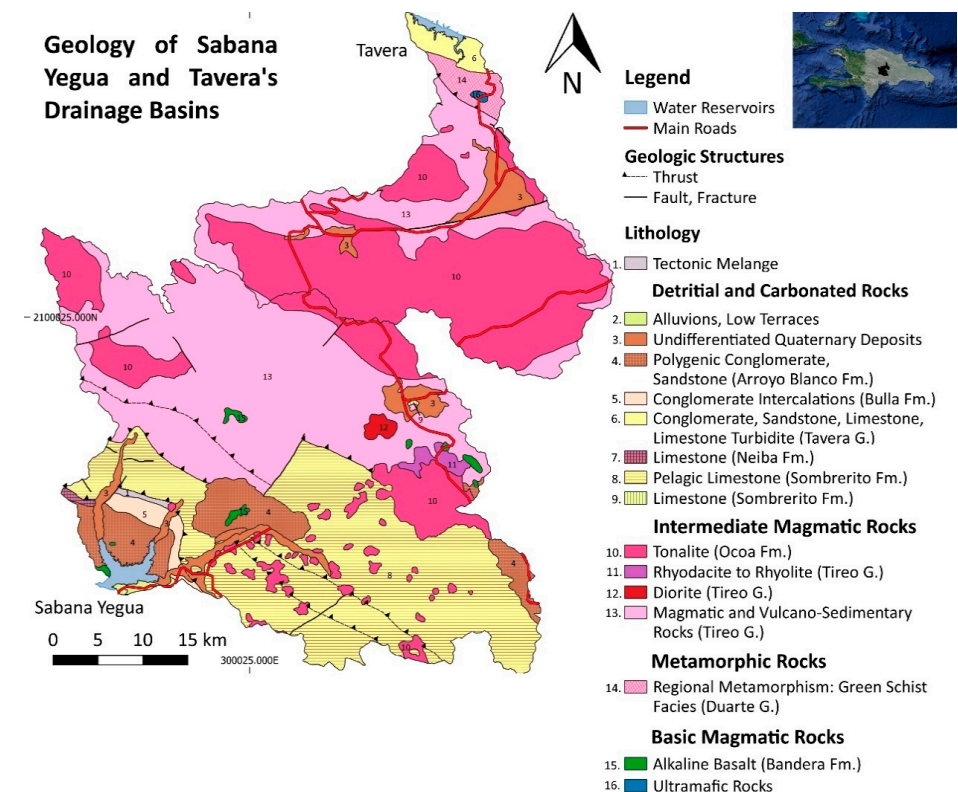


Figure 1. Geological map of Sabana Yegua and Tavera's drainage basins.

3. Methodology

3.1. Sampling

The grid for soil sampling was selected according to the most representative lithologies of each catchment previously studied by [25–27], the topography of the region, and the sub-catchments of all tributaries (Table 1). Sampling was carried out in a field campaign after the rainy season (February 2017) using a manual auger, which allows the removal of about 20 cm of soil thickness. At each sampling point, three sub-samples of the first soil layer were collected and homogenized to obtain a more representative sample.

Table 1. Soils studied and their corresponding parent rocks in the Sabana Yegua and Tavera catchments. The petrographic characterization/identification of the rocks was presented in [26,27].

Sabana Yegua Basin		Tavera Basin	
Soils	Correspondent Rocks	Soils	Correspondent Rocks
SYS1	Intermediate Igneous Rocks (Granodiorite)	TS1	Detrital Rocks (conglomerates, sandstones)
SYS2; SYS6	Intermediate Igneous Rocks (Dacite, Andesite)	TS2, TS3	Mafic Igneous Rocks (Olivinic Norite)
SYS3	Detrital Rocks (conglomerates, sandstones)	TS4, TS5, TS6, TS7	Intermediate Igneous Rocks (Tonalite)
SYS4	Mafic Igneous Rocks (Basalts)	TS8	Mafic Igneous Rocks (Gabbro)
SYS5, SYS7	Intermediate Igneous Rocks (Tonalite)		
SYS8, SYS9	Carbonate Sedimentary Rocks		

Surface sediments (approximately 20 cm thick) were collected throughout the lakes area using a small Shipeck dredge suitable for small boats. To determine if the distribution of concentrations and patterns of REE change throughout the year, surface sediments were sampled in two separate field campaigns, after the main rainy season (February 2017) and after the dry season (July 2017), at points distributed throughout the reservoirs to include areas with different depths (Table 2), under the influence of all tributaries, and with a greater diversity of hydrodynamic conditions. These samples were selected from the geochemical data of major and minor elements obtained in previous studies by [25–27] on samples from a wider sampling network. In these studies, different clusters were defined and one sample from each was selected for REE analysis in the present study. Each sample resulted from the mixture of three subsamples collected at nearby points. The location of the sampling points for soils and sediments (second campaign) is shown in Figure 2.

Table 2. Depth of the sediments samples included in the geochemical study of REE in both seasons: rainy season (February) and dry season (July).

Sabana Yegua Reservoir				Tavera Reservoir			
Samples	Depth (m) July 2017	Samples	Depth (m) July 2017	Samples	Depth (m) February 2017	Samples	Depth (m) July 2017
(February 2017)		(July 2017)		(February 2017)		(July 2017)	
SY2	50	SY1	43	T1	46.3	T1	42
SY3	43	SY3	39	T5	27.5	T2	32
SY9	37.3	SY4	20	T8	9	T3	24
SY10	27.8	SY5	35	T12	23	T4	19.6
SY11A	14	SY6	9			T5	22
SY13	18	SY7A	21.5			T6	15
SY14	7	SY8	8			T7	3.2
		SY9	29			T9	18
		SY10	20			T10	28.6
		SY13	13.8			T11	23.8
		SY14	4			T12	27.1
		SY15	15			T13	42

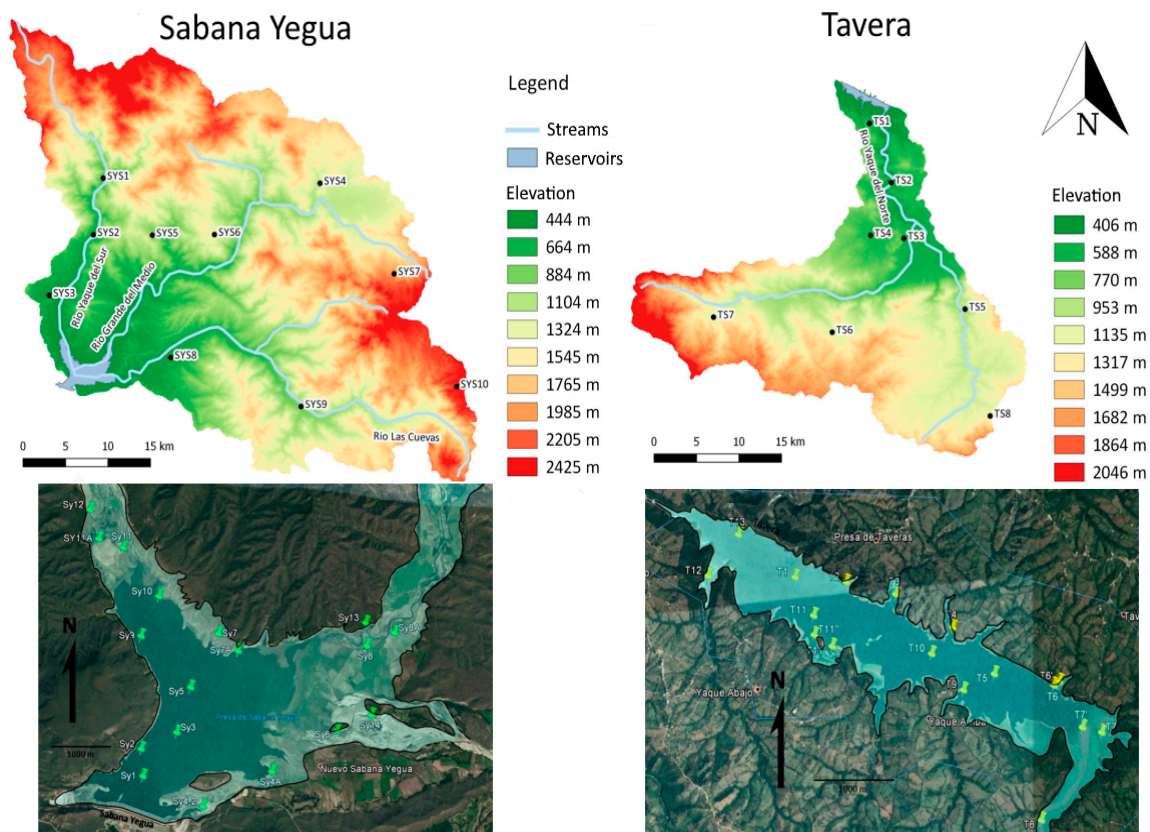


Figure 2. Distribution of sediment and soil samples selected for REE analysis in Sabana Yegua and Tavera’s reservoirs and in their catchments.

After sediments and soils were collected, the Eh and pH values in the wet samples were measured immediately using a portable multiparameter Consort, model C5020, with the following probes: model SP10T for pH, model SP50X for redox potential. For soil samples whose moisture was insufficient for direct pH measurement, this parameter was measured in the laboratory in a soil–water suspension (1:2.5). From the time of collection, the samples were kept at about 4 °C for geochemical analysis.

3.2. Analytical Methodologies

To identify the sediment sources of both reservoirs, geochemical investigation of REE was carried out in the sediments of both seasons and in the soils from their catchments. The data from both groups of samples were compared with the geochemical data from REE of the rocks of the catchments obtained by [25,26] and are presented in Table 3.

Table 3. Concentration of rare earth elements (REE) in rocks of Sabana Yegua and Tavera basins. (*—The asterisk is used to indicate anomalies.)

Samples	Lanthanides											Total	Ratio	Normalized Values To NASC					Classification					
	LREE (μgg^{-1})					HREE (μgg^{-1})			Other REE (μgg^{-1})					Σ REE	LREE/HREE	(La/Yb) _N	(La/Sm) _N	(La/Gd) _N		(Gd/Yb) _N	Eu/Eu*	Ce/Ce*		
ULTRAMAFIC IGNEOUS ROCKS																								
2-T4	10.244	20.091	0.806	10.764	1.749	0.445	2.084	0.750	0.138	1.338	0.842	0.173	5.703	65.498	0.136	49.425	8.28	1.178	1.043	0.799	1.475	1.024	1.523	Gabbroic cumulate
2-T8	16.616	23.274	4.746	19.167	3.804	1.121	3.176	5.196	0.390	1.815	0.944	0.109	12.129	73.145	0.755	80.358	5.91	1.705	0.778	0.850	2.006	1.416	0.571	Gabbroic cumulate
2-T11	3.280	21.311	<0.1	8.239	2.146	0.882	3.096	5.790	0.827	2.372	2.563	0.339	22.390	46.058	1.449	50.845	2.39	0.124	0.272	0.172	0.720	1.502	8.105	Websterite
MAFIC IGNEOUS ROCKS																								
1-S1	39.996	64.474	5.978	29.402	4.072	1.171	3.600	2.726	0.521	2.077	2.038	0.366	18.993	20.199	3.119	156.422	12.81	1.901	1.749	1.805	1.053	1.343	0.908	Basalt
1-S3	36.957	66.113	8.490	36.297	5.741	1.598	3.982	3.427	0.594	1.984	1.946	0.333	18.411	26.376	2.743	167.464	12.65	1.840	1.147	1.508	1.220	1.467	0.813	Basalt
2-S4	22.800	40.198	3.848	22.628	3.569	1.042	3.236	2.616	0.496	1.917	1.823	0.311	16.242	31.578	2.539	104.484	9.05	1.211	1.138	1.145	1.058	1.346	0.935	Basalt
2-S6	8.228	17.852	0.110	9.363	1.391	0.428	2.082	0.941	0.187	1.186	1.038	0.203	7.254	25.866	0.585	43.009	6.63	0.768	1.054	0.642	1.195	1.105	4.080	Basalt
2-T5	8.072	16.661	0.120	9.619	1.968	0.662	3.082	3.225	0.638	2.460	2.333	0.382	18.552	47.489	0.573	49.220	3.06	0.335	0.731	0.426	0.788	1.180	3.694	Olivinic Norite
2-T12A	1.217	18.879	<0.1	6.247	1.432	0.672	2.330	5.433	0.611	2.125	1.959	0.256	17.817	38.233	1.323	41.162	2.24	0.060	0.151	0.085	0.709	1.615	11.789	Basalt
2-T14	7.286	26.808	1.748	14.281	3.647	1.083	4.801	6.558	1.309	2.837	4.040	0.546	34.083	23.799	3.831	74.943	2.73	0.175	0.356	0.247	0.708	1.136	1.636	Gabbro
2-T12	3.462	18.507	0.664	10.463	2.998	1.179	3.767	6.005	0.938	2.536	2.880	0.388	25.577	46.937	1.146	53.785	2.26	0.116	0.206	0.149	0.780	1.540	2.659	Vesicular Basalt
INTERMEDIATE IGNEOUS ROCKS																								
1-S2	32.162	54.075	6.457	28.556	4.274	1.245	3.264	2.714	0.488	1.779	1.834	0.315	14.521	19.587	3.060	137.163	12.20	1.699	1.341	1.601	1.061	1.464	0.817	Andesite
2-S2	17.292	37.973	4.064	26.306	6.963	1.883	8.279	11.503	2.143	5.334	6.204	0.911	56.870	39.879	5.929	128.856	2.75	0.270	0.442	0.339	0.796	1.089	0.987	Phonolitic Tephrite
2-S5	33.441	57.427	6.133	26.563	3.935	1.140	2.850	2.101	0.372	1.508	1.424	0.251	11.103	19.304	2.599	137.146	15.12	2.275	1.514	1.907	1.193	1.495	0.873	Foidite
2-S7	8.525	16.954	<0.1	9.216	1.366	0.408	2.055	0.893	0.182	1.326	1.023	0.206	7.238	24.403	0.440	42.155	6.41	0.807	1.112	0.674	1.198	1.068	3.999	Dacite
2-S8	11.393	21.524	0.909	11.357	1.914	0.553	2.345	1.207	0.225	1.335	1.092	0.216	7.811	15.941	0.691	54.069	7.42	1.010	1.060	0.790	1.280	1.145	1.457	Andesite
2-S9	17.634	36.611	3.306	19.569	3.603	1.136	3.489	2.942	0.515	1.834	1.708	0.294	15.508	8.577	2.244	92.641	7.59	1.000	0.872	0.821	1.218	1.407	1.044	Quartz Monzonite
2-S3	10.451	18.216	0.488	10.866	2.026	0.660	2.793	1.952	0.363	1.537	1.301	0.231	10.511	10.115	2.567	50.884	5.22	0.778	0.919	0.608	1.280	1.218	1.757	Trachyandesite
1-T2	14.442	27.377	1.442	13.615	2.176	0.656	2.387	1.237	0.238	1.335	1.096	0.216	7.926	12.968	1.931	66.216	9.17	1.277	1.182	0.983	1.298	1.263	1.307	Tonalite
1-T3	13.562	27.628	1.568	13.938	2.333	0.769	2.560	1.540	0.281	1.390	1.239	0.231	9.090	24.585	1.062	67.038	8.26	1.061	1.036	0.861	1.232	1.381	1.305	Tonalite
2-T6	26.799	40.067	3.963	19.694	2.727	0.480	2.329	1.170	0.254	1.225	1.276	0.246	7.817	4.879	2.995	100.230	14.42	2.035	1.751	1.870	1.088	0.836	0.847	Granodiorite
2-T7	22.618	40.918	3.371	19.035	3.058	0.842	2.687	1.619	0.298	1.435	1.254	0.233	9.485	10.014	1.960	97.369	11.94	1.747	1.317	1.368	1.277	1.290	1.021	Tonalite
2-T9	5.699	24.394	0.865	10.972	2.349	0.868	2.489	5.145	0.391	1.809	1.063	0.133	12.106	30.897	1.516	56.177	4.09	0.519	0.432	0.372	1.396	1.576	2.393	Tonalite
2-T9A	5.643	24.006	0.977	10.532	2.018	0.723	1.985	5.000	0.315	1.886	1.043	0.134	10.577	68.439	1.005	54.261	4.24	0.524	0.498	0.462	1.135	1.586	2.226	Granodiorite
2-T13	17.073	40.560	5.583	22.405	4.729	0.612	4.080	5.709	0.687	2.235	2.080	0.275	20.274	4.152	3.183	106.027	6.04	0.795	0.643	0.680	1.169	0.612	0.905	Muscovitic Tonalite
METAMORPHIC ROCKS																								
1-T1	6.241	11.259	<0.1	5.018	0.497	0.058	1.194	0.753	0.341	0.820	0.520	0.136	1.999	10.075	4.999	26.835	6.13	1.162	2.239	0.850	1.367	0.328	3.104	Serpentinite
2-T9B	2.072	18.910	<0.1	6.276	1.276	0.568	1.633	4.864	0.236	1.619	0.690	0.080	8.747	71.244	1.047	38.224	3.19	0.291	0.289	0.206	1.412	1.728	9.049	Hornblende Schist
2-T10	4.072	22.013	<0.1	8.360	1.885	0.813	2.719	5.537	0.679	2.217	2.164	0.296	19.618	34.280	1.437	50.757	2.73	0.182	0.385	0.243	0.749	1.577	7.514	Green Schist
VOLCANO SEDIMENTARY ROCKS																								
2-S1	10.402	28.588	0.965	13.484	2.780	0.936	3.412	3.264	0.595	2.071	2.004	0.327	17.289	36.936	1.479	68.829	4.90	0.503	0.666	0.495	1.015	1.334	1.965	Volcano-sedimentary
2-S1A	10.962	24.558	1.444	13.979	2.909	0.990	3.567	3.363	0.615	2.082	2.082	0.341	18.162	40.368	2.928	66.893	4.55	0.510	0.671	0.499	1.022	1.350	1.345	Volc. sed. Breccia
CARBONATE SEDIMENTARY ROCKS																								
3-S10	47.015	4.717	1.113	3.217	0.487	0.237	0.681	<0.1	0.154	<0.1	0.205	0.136	7.572	1.331	<0.1	57.963	48.27	22.193	17.188	11.215	1.979	1.803	0.142	Limestone
3-S11	65.850	12.256	2.377	8.824	1.857	0.447	1.886	1.568	0.310	0.368	0.853	<0.1	11.789	15.656	1.079	96.597	18.37	7.476	6.315	5.674	1.317	1.048	0.213	Carbonate Breccia

Grain size analysis of soils and sediments was carried out by separating grain size classes (Wentworth–Lane scale for sediments and Atterberg scale for soils [28]) by wet sieving (gravel:sand:silt–clay) and pipetting using the Anderson pipette method to separate the two fine-grained particles, silt and clay [29]. The proportions of the clay, silt, and sand fractions of the sediments were plotted on a triangular diagram by Shepard (1954) [28] and the data of the soils were plotted on a USDA soil texture diagram (Natural Resources Conservation Service Soils, USA), allowing the subsequent textural classification of both.

Geochemical analyses were performed on powdered samples in an agate ring mill up to a mesh size of 200. Soil analyses were performed on the <2 mm soil fraction, which was assumed to have negligible metal and REE composition.

For the analysis of REE, the soil and sediment samples were melted in platinum crucibles with an alkaline flux of lithium metaborate (ratio 1:4) in a muffle furnace at 1000 °C, followed by dissolution of the obtained glass beads in a hydrochloric acid solution according to [30–32]. Most interfering elements were eliminated by cation exchange using an ion exchange column filled with BioRad AG50W-X8 resin (H⁺ form, 200–400 mesh) with adjusted acidity. REE separation involved sequential elution of cations adsorbed to the resin through a gradient of low-concentration nitric and hydrochloric acid solutions, isolating REE from matrix elements. In addition to REE, Y, Sc, Hf, and Zr were also retained in the column, and were subsequently extracted with highly concentrated acid solutions (HNO₃ and HCl). The solution containing REE was evaporated to dryness and dissolved with nitric acid solution immediately before analysis.

The contents of REE, Y, Sc, and Hf were analyzed by optical emission spectroscopy using an inductive plasma source (ICP-OES, Perkin-Elmer OPTIMA 8300) operated under the following conditions: plasma gas flow—10 L/min; auxiliary gas flow—0.2 L/min; atomizer gas flow—0.55 L/min; sample flow—1.50 mL/min; RF power—1450 watts; atomizer (PFA-ST3 Microflow atomizer)—0.1–3 mL/min; viewing modes—radial and axial; read time—2–5 s; read delay—60 s; high resolution. Indium was chosen as the internal standard. Under the optimal experimental conditions, the detection limits for the REE ranged from 0.01 µg g⁻¹ (Yb, Eu, Lu), 0.02 µg g⁻¹ (Dy, Sc, Hf), 0.03 µg g⁻¹ (Ho, Er), 0.05 µg g⁻¹ (La, Gd, Y), to 0.1 µg g⁻¹ (Ce, Pr, Nd, Sm). Spectral interferences between some rare earths and with Zr were eliminated by interelement correction factors (IEC) calculated based on the analysis of monoelement interference control standards.

For quality control, all chemical methods were tested with analytical replicates, two blanks prepared by the same analytical methods, and certified reference materials (CRMs) with an accuracy of R < 5%: NIM -L (MINTEK, South Africa), JR -3 and JA -2 (GSJ, Japan), GSR-1 and GSR-5 (IGGE IRMA, China). The proportion of multielement quality control (QC) solution was less than 2% and CRMs were performed every 10 samples.

3.3. Rare Earth Element Data Processing and Geochemical Parameters

To avoid the Oddo–Harkins effect [9,12,15], the REE contents of soils and sediments were normalized to North American Shale Composite (NASC) according to the values suggested by [7], where N used in this study means the normalized values for NASC. The same normalization was performed for the rocks of the basins studied by [25,26]. According to several authors [9,33], an “average sediment” is generally used as a normalization value for REE concentrations in sedimentary rocks and sedimentary deposits in marine and continental environments because the concentration of many elements in fine-grained sedimentary rocks is similar due to mixing by repeated erosion cycles. Normalization of soils and rocks to a composite shale reference standard should allow identification of enrichment or depletion of an element or group of elements in sediments relative to parent materials and comparison of fractionation parameters among the three components.

For soils and sediments, quantification of the La–Lu series, Y, Sc, and Hf, the ratio between LREE (light REE: La–Sm) and HREE (heavy REE: Gd–Lu), REE fractionation parameters, anomalies of Eu (Eu/Eu*) and Ce (Ce/Ce*), and NASC-normalized spider

diagrams of the La–Lu series and elements with similar behavior (Y, Sc, Hf) were used as proxies to define the sources of sediments deposited in the two reservoirs. This definition of the sources was made possible by comparing the REE data of the sediments and the same data obtained for the soils and rocks of the basins.

The REE fractionation parameters were determined by correlating between the NASC-normalized concentrations: $(La/Yb)_N$, $(La/Sm)_N$, $(La/Gd)_N$, and $(Gd/Yb)_N$. The ratios $(La/Yb)_N$ and $(La/Gd)_N$ are a measure of the enrichment of LREE relative to HREE, while $(La/Sm)_N$ defines the fractionation of LREE, and $(Gd/Yb)_N$ defines the fractionation of HREE [18,23]. The europium (Eu^*) and cerium (Ce^*) anomalies were calculated based on the equations given in [7]:

$$Eu/Eu^* = Eu_N / (Sm_N \times Gd_N)^{1/2}$$

$$Ce/Ce^* = Ce_N / (La_N \times Pr_N)^{1/2}$$

For each reservoir, bivariate plots of ΣREE , LREE/HREE, Ce/Eu anomalies, and fractionation parameters ($(La/Yb)_N$, $(La/Sm)_N$, $(La/Gd)_N$, $(Gd/Yb)_N$), including sediments from both sampling periods and soils and rocks from the catchments, were used as tracers to determine the origin of the sediments. Using RStudio software (Version 1.2.5019) and the ggplot and ggforce modules, an ellipse was drawn in each plot to delineate the points of soils and rocks near the sediment points. The soils and rocks included in this ellipse have the highest correlation values with respect to these sedimentary materials and represent their main sources. These ellipses were drawn based on the Krachyan algorithm for a tolerance level of 0.95 [34].

Kriging interpolation maps created with SURFER software12 were used to visualize the spatial distribution of REE in both reservoirs. Collecting and analyzing sufficient data for variogram estimation is often expensive and a problem when working with a limited budget. Nevertheless, it is satisfactory to assume that given the small area of the lakes (21 km² for Sabana Yegua and 6.20 km² for Tavera) and the environmental variables, the fitted models of the selected variograms can be enriched by experts [35–37]. Therefore, for the calculation of the interpolation, the ordinary kriging algorithm was applied and spherical isotropic variograms were fitted, assuming as total variance the calculated variance for each variable and a range of 7 km², since the variogram values can be expected to stop changing and reach a “plateau” due to the known endogenous (geological) and exogenous (contributions) characteristics.

4. Results and Discussion

This study presents a detailed analysis of REE fractionation patterns in the sediments of the Sabana Yegua and Tavera reservoirs and the soils of their catchments, with the aim of better understanding the behavior and spatial and seasonal distribution of these elements in tropical systems under the influence of high annual rainfall rates. These data will also help to provide a first clue for the identification of the main sources of sediments overaccumulated in the two reservoirs, by comparing the geochemical data of REE with those of the soils and rocks in the catchments. The REE geochemistry of the rocks was previously analyzed and presented in [25,26] and is summarized in Table 3.

4.1. Distribution of Rare Earth Elements in the Soils of the Drainage Basins

In both catchments, soils have similar REE patterns and anomalies of Ce and Eu, with few exceptions (Table 4; Figure 3). Although the soils are depleted in LREE compared to the upper continental crust [7], normalized values of soils to the North American Shale Composite (NASC) show REE patterns slightly enriched in LREE (La to Nd), with variable ratios $(La/Yb)_N$ ranging from 0.128 to 0.954, indicating a significant concentration of heavy minerals that may represent the main pool of these elements in the soils.

Table 4. Concentration of rare earth elements (REE), anomalies of Eu and Ce, and fractionation parameters in soils of Sabana Yegua and Tavera basin. (*—The asterisk is used to indicate anomalies.)

Concentration of Rare Earth Elements (REE) in the Soils of Sabana Yegua and Tavera's Basins													
SAMPLES	LREE						HREE						
	La	Ce	Pr	Nd	Sm	Eu	Gd ($\mu\text{g g}^{-1}$)	Dy	Ho	Er	Yb	Lu	Y
SYS1	21.13	54.07	6.56	29.58	6.64	1.79	6.26	4.86	0.81	2.58	2.15	0.40	26.16
SYS2	5.66	22.17	1.07	8.83	1.73	0.60	2.06	2.60	0.35	2.25	1.43	0.34	10.98
SYS3	14.10	34.59	3.76	17.29	3.82	1.00	3.80	3.65	0.58	2.54	2.01	0.40	19.44
SYS4	0.05	10.32	0.68	6.73	2.04	0.77	2.89	3.50	0.55	2.52	2.06	0.40	18.81
SYS6	2.52	15.79	1.08	8.54	2.14	0.78	2.81	3.36	0.51	2.52	1.91	0.38	16.39
SYS8	10.91	20.82	2.78	12.31	2.81	0.88	3.10	2.67	0.59	1.18	1.50	0.23	14.89
SYS9	15.84	28.44	3.67	15.33	3.24	0.99	3.30	2.73	0.63	1.31	1.64	0.26	15.51
SYS10	10.05	19.36	2.10	11.09	2.43	0.73	2.72	2.33	0.50	1.03	1.22	0.20	11.20
TS1	1.42	12.99	1.04	8.07	1.64	0.62	2.63	4.14	0.77	2.86	2.50	0.41	27.64
TS3	9.88	27.51	1.39	11.83	2.62	0.80	3.05	2.85	0.39	1.50	1.24	0.33	13.46
TS5	9.81	29.70	2.86	13.00	3.66	0.95	3.49	2.84	0.36	1.92	1.46	0.28	14.33
TS6	3.81	13.65	0.90	9.29	2.24	0.74	2.51	2.53	0.24	0.73	0.81	0.28	8.33
TS7	3.25	15.12	0.80	7.75	1.60	0.66	1.80	2.10	0.17	1.70	0.61	0.25	4.95
TS8	5.48	16.28	0.59	8.09	0.93	0.37	1.70	1.90	0.32	1.36	1.09	0.27	5.53

SAMPLES	Sc	Hf	Σ REE ($\mu\text{g g}^{-1}$)	LREE/HREE	NORMALIZED VALUES TO NASC				TEXTURE (%)				
					(La/Yb) _N	(La/Sm) _N	(La/Gd) _N	(Gd/Yb) _N	Eu/Eu*	Ce/Ce*	Sand	Silt	Clay
SYS1	33.60	5.31	136.82	7.02	0.95	0.57	0.55	1.74	1.22	1.00	68	18	14
SYS2	18.61	4.44	49.09	4.44	0.38	0.58	0.45	0.86	1.40	1.96	24	28	48
SYS3	22.99	2.75	87.54	5.75	0.68	0.66	0.60	1.13	1.15	1.03	66	16	18
SYS4	48.28	1.23	32.50	1.73	0.00	0.00	0.00	0.84	1.40	12.35	47	25	28
SYS6	42.69	1.76	42.34	2.68	0.13	0.21	0.15	0.88	1.39	2.08	36	32	32
SYS8	27.01	2.15	59.78	5.45	0.70	0.69	0.57	1.23	1.31	0.82	40	34	26
SYS9	24.80	2.31	77.38	6.84	0.94	0.87	0.78	1.20	1.33	0.81	40	32	28
SYS10	27.48	2.10	53.76	5.71	0.80	0.74	0.60	1.33	1.25	0.92	26	52	22
TS1	45.84	2.45	39.10	1.94	0.06	0.15	0.09	0.63	1.31	2.33	27	35	38
TS3	18.39	4.08	63.42	5.77	0.77	0.67	0.53	1.46	1.24	1.62	38	43	19
TS5	20.25	3.21	70.33	5.79	0.65	0.48	0.46	1.43	1.17	1.22	50	23	27
TS6	32.96	1.53	37.73	4.32	0.46	0.30	0.25	1.85	1.38	1.61	47	27	26
TS7	23.91	1.89	35.79	4.41	0.52	0.36	0.29	1.76	1.71	2.04	37	29	34
TS8	35.40	3.41	38.38	4.78	0.49	1.05	0.52	0.93	1.31	1.97	14	21	65

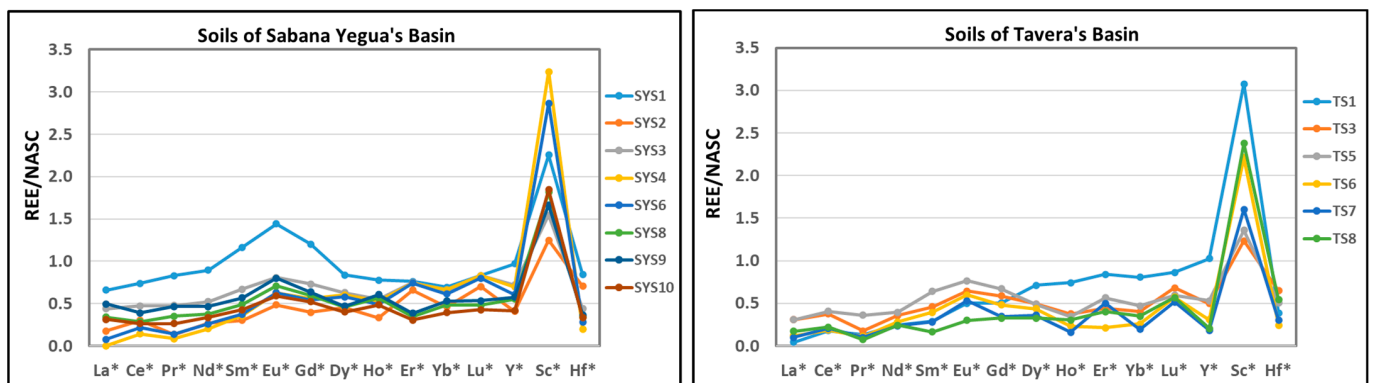


Figure 3. Spider diagrams of the soils from Sabana Yegua and Tavera basins.

In Tavera basin, due to the greater geological homogeneity, the soils show a much higher uniformity in terms of total concentration and distribution patterns of REE compared to those of Sabana Yegua. In this latter basin, only Y is uniformly distributed in the soils.

Although most authors [7,21,38,39] point to the enrichment of REE with the increase of finer particles, the correlation between the sum of REE and the texture is only found in the soils of Tavera, where the nature of rocks is more homogeneous and most of the studied soils derive from tonalitic rocks. In this basin, the total amount of REE is proportional to

the silt concentration ($r > 0.6$), the fraction with which REE are preferentially associated in the soils, according to [40,41]. In the Sabana Yegua basin, the higher lithological diversity overrides the effect of particle size, and there is no significant relationship with texture. Contrary to [7], there is also no significant relationship between the fractionation parameters of LREE and HREE, Ce and Eu anomalies, and the contents of the sandy, silty, or clay fractions of the soils in both basins. The variation of some fractionation parameters, such as $(La/Yb)_N$, rather reflects the petrographic nature of the source rocks. The lowest values of this parameter are found in soils influenced by basic rocks, such as TS1 (soil from conglomerates with abundant basic rocks), TS8 (soil influenced by gabbros), and SYS4 (soil influenced by basalts).

Soils are an important sink for REE, and their concentrations are mainly governed by the parent material and pedogenic processes [42]. To try to understand the distribution and behavior of REE in soils with distinct sources, soils were grouped according to the geological group of the parent rocks.

4.1.1. Soils Derived from Igneous Rocks

(1) Soils derived from intermediate igneous rocks: This group includes soils formed in tonalitic rocks—Tavera basin (TS5, TS6, TS7, and TS8) and Sabana Yegua (SYS1). By comparing them, there is a remarkable enrichment of the total contents of REE in the soil of Sabana Yegua, which is under the influence of a quartz monzonite ($\Sigma REE = 136.8 \mu g g^{-1}$). This enrichment particularly affects the lighter elements (LREE), resulting in higher values of the LREE/HREE ratio (7.0) and higher values of the fractionation parameters $(La/Yb)_N$, $(La/Sm)_N$, and $(La/Gd)_N$. The remaining soils in this group have ΣREE ranging from 27.34 and $70.33 \mu g g^{-1}$ and LREE/HREE ratios from 3.77 to 5.79.

(2) Soils derived from magmatic and volcanic sedimentary rocks: This heterogeneous group includes three soils from Sabana Yegua basin (SYS2, SYS4, SYS6) and one from the Tavera basin (TS3), three of them with influence of other lithologies, apart from the main sources: intermediate igneous rocks (SYS2) and basic rocks (SYS4—basalt; TS3—norite). Comparing the contents of REE with the data of the rocks from the basin (Table 3), the soil of Tavera (TS3) is the one that has the total concentration of REE, the distribution patterns, and the Ce and Eu anomalies identical to this group of source rocks, with only a slight depletion of HREE. There is also a marked loss of Sc and a small increase in Hf. In this group, this soil has the finest texture expressed by the highest silt content, which could explain the REE enrichment that goes beyond the inheritance of REE-rich basic rocks. Texture is indeed a very important factor in the enrichment or depletion of these elements in this soil group, since there is a proportionality between the content of REE and the fine-grained particles; the increasing order of the percentage of the silty and clayey fraction of the soils (SYS4 \rightarrow SYS6 \rightarrow SYS2 \rightarrow TS3) is accomplished by the increase of ΣREE : $32.50 \mu g g^{-1} \rightarrow 42.34 \mu g g^{-1} \rightarrow 49.09 \mu g g^{-1} \rightarrow 63.42 \mu g g^{-1}$.

The soil developed on basalts (SYS4) has a coarser texture and appears to have no relationship to this basic rock in terms of REE pattern: (1) a pronounced REE depletion, probably as a result of the dilution effect of quartz, and (2) a distinct distribution pattern, characterized by a pronounced depletion of La and a moderate depletion of Ce, Pr, and Nd, implying a decrease in the LREE/HREE ratio (and in the parameters $(La/Yb)_N$, $(La/Sm)_N$, and $(La/Gd)_N$) and a very high Ce/Ce* anomaly (12.350).

The remaining soils, SYS2 and SYS6 are similar in terms of the distribution pattern of the La–Lu series, the total concentration of REE, and the Eu and Ce anomalies. Compared to the magmatic and volcano sedimentary rocks of the basin (Table 3), both soils are generally depleted in La and Nd, but have similar contents of the remaining elements and similar anomalies of Ce and Eu, suggesting inheritance from these rocks.

The average LREE concentrations in igneous rock soils, similar to soils in Cuba [43], are lower than values reported for soils in other countries, such as Brazil, Japan, China, and Europe [44–48], and the average $\Sigma HREE$ is higher. The differences in terms of LREE/HREE ratio are probably due to the low occurrence of felsic rocks in these Caribbean islands, as

LREE tend to be higher in felsic rocks and lower in mafic rocks [49]. The lack of felsic rocks in the basins of these reservoirs can also explain the low contents of La, which has the third largest concentration after Ce and Nd; this is because La is widely distributed in trace amounts in several rock-forming minerals, mainly feldspar, biotite, and apatite, which are common in felsic rocks, and has a lower affinity for mafic, ultramafic, and metamorphic rocks [50].

In both basins, Ce and Eu anomalies in soils derived from igneous rocks are always positive, reflecting the inheritance of the positive anomalies from basin rocks [25,26], but they are higher than the corresponding values in rocks, probably due to the oxidative conditions of the soils.

4.1.2. Soils Derived from Detrital and Carbonate Sedimentary Rocks

(1) Soils derived from detrital sedimentary rocks: This group includes a soil in the Tavera basin on conglomerates, sandstones, and reef limestones (TS1) and (2) a soil in Sabana Yegua on a tectonic mélange of detrital and carbonate rocks with intercalations of conglomerates (SYS3). Although these soils were formed on similar sedimentary rocks, they have quite different REE distribution patterns among themselves and in relation to the soils of the other groups. The fine-grained soil of Tavera is depleted in REE, significantly enriched in HREE, Y, and Sc, and depleted in LREE (La and Ce), resulting in a low LREE/HREE ratio of 1.94 and very low fractionation parameters $(La/Yb)_N$, $(La/Sm)_N$, and $(La/Gd)_N$, while the soil of Sabana Yegua is a coarse soil with high values of REE. The distribution of lanthanides, Y, Sc, and Hf is very similar to that of soils from carbonate rocks, differing only by a slight decrease in the Eu anomaly and a slight increase in the Ce anomaly, which becomes zero.

(2) Soils derived from carbonate sedimentary rocks: They occur only in the basin of Sabana Yegua (SYS8, SYS9, SYS10). Unlike the other groups, the carbonate soils are very homogeneous among themselves in terms of the values and distribution of REE and the Ce and Eu anomalies: (Eu/Eu*: 1.25–1.33 and slight negative Ce anomalies: 0.81–0.92). These soils show significant differences from igneous-derived soils in (1) higher concentrations in La, Ce, and Sm, (2) higher LREE/HREE ratios (5.45–6.84), and (3) higher fractionation parameters $(La/Yb)_N$ and $(La/Sm)_N$, with values above 0.7, reflecting the preponderance of light elements. The enrichment in LREE, in relation to the other soils, could be due to the binding of REE (especially LREE) to CO_3 , resulting in REE carbonates which precipitate easily at the high pH values of these soils (pH > 7.6) [45].

A comparative analysis of the distribution of REE between this group of soils and the carbonate rocks of the basin (Table 3) shows that the Ce anomaly and the total concentration of REE are maintained, but there is a strong variation in the distribution patterns of most elements, with a marked decrease in La and an enrichment of Ce, Nd, Sm, and Eu in the soils. There is also a moderate increase in the other elements of the MREE and HREE series in the soils, resulting in significantly lower LREE/HREE ratios. The slightly negative Ce anomaly in these soils, which has also been observed in soils from other Caribbean regions [43], can be explained by the release of clays in which the oxidized Ce^{4+} is preferentially retained during the dissolution of carbonates.

In this study, the chemistry of REE in soils rarely reflects the patterns of the source rocks, except in soils from carbonate rocks. In most soil types, there is a slight enrichment of middle (MREE) and heavy REE (HREE), and a depletion of LREE, especially La. Although many authors [43,44,46,51,52] have observed a decrease in the natural contents of REE in soils derived from rocks in the following order: granite > basalt > limestone > sandstone, and that the presence of quartz can affect the concentration of these elements due to its dilution effect [7,21,38–40,42], the sum of all lanthanides (ΣREE) in the soils of Tavera and Sabana Yegua basins with identical parent rocks does not behave uniformly and does not follow the lithological order indicated above; the highest concentrations correspond to either soils derived from tonalitic rocks or those derived from detrital deposits and carbonate rocks.

On the other hand, tonalitic rocks, the main sources of these soils, particularly in Tavera basin, give rise to soils with a wide range of Σ REE contents, from $27.34 \mu\text{gg}^{-1}$ to $136.82 \mu\text{gg}^{-1}$.

The variability of the REE distribution in soils evidences the inheritance from a mixture of lithotypes of different nature scattered in the most representative rocks of the basins, or outcropping in upstream areas with higher gradients, that are therefore easily eroded and incorporated into the soils. The geochemical mobility of REE from those rocks is enhanced by the high precipitation rate and temperature, resulting in high weathering and leaching rates and hydraulic sorting processes [3]. While LREE preferentially occur as free species and are more strongly retained, HREE are more mobile and leachable from the rocks, forming easily soluble complexes with, e.g., amorphous Fe–Mn oxides, organic matter, and carbonates in the weathered environment [22,52], which may explain the moderate HREE increase in these soils. The enrichment in HREE can also be explained by the relationship between the pH values of soils and the concentration of REE. In the pH range of these soils, i.e., above 6, the surface of soil particles and organic matter is more negatively charged, which facilitates adsorption, and the REE species tend to complex, especially HREE, increasing the retention level by forming inner sphere complex complexes [15,52].

4.2. Rare Earth Elements in the Reservoir’s Sediments

The chemistry of REE in sediments is consistent in space and time. There are no significant differences between different sampling sites or between sampling periods, indicating high homogeneity in the sedimentation process of these systems, even in distinct seasonal periods (Table 5 and Figure 4).

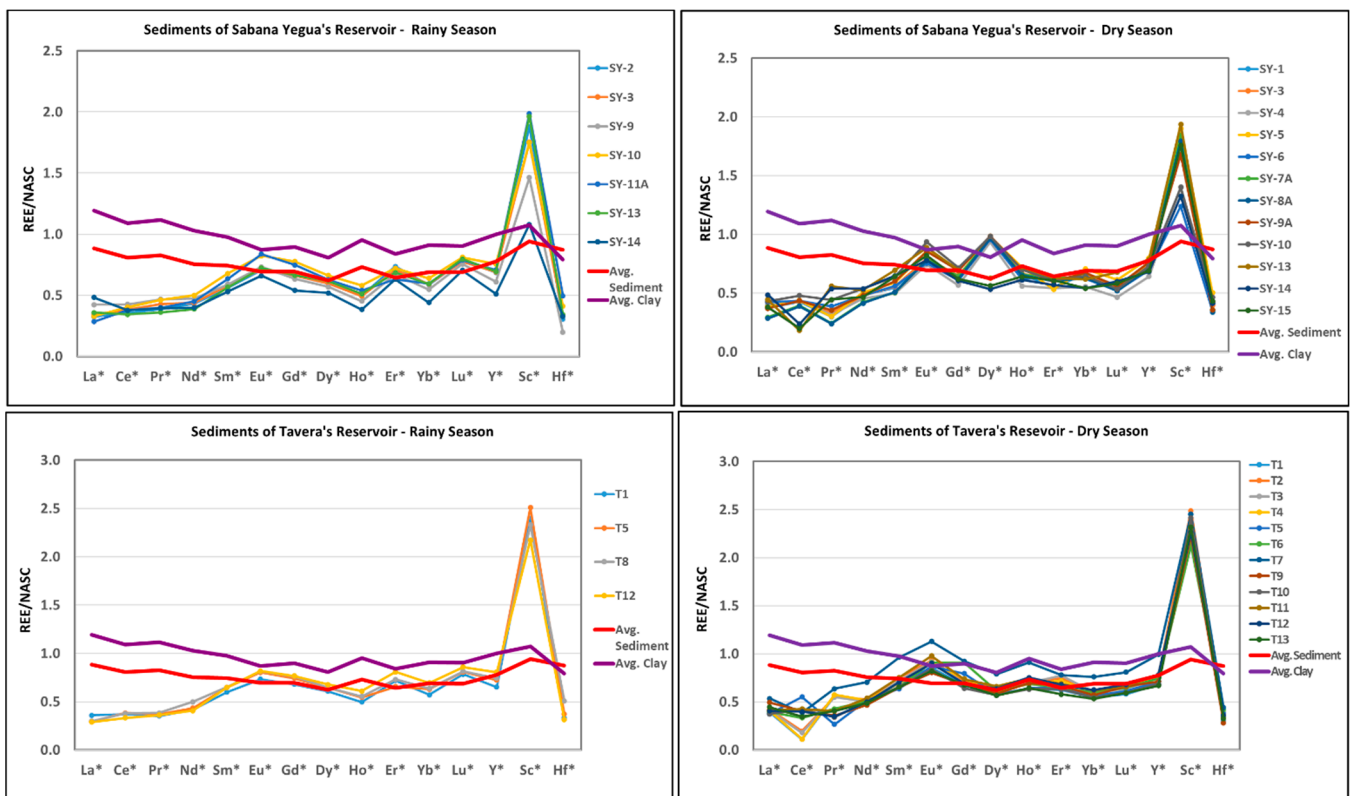


Figure 4. Spider diagrams of the sediments from Sabana Yegua and Tavera’s reservoirs in two seasonal periods.

Table 5. Concentration of rare earth elements (REE), anomalies of Eu and Ce, and fractionation parameters in the sediments of Sabana Yegua and Tavera’s reservoirs in two seasonal periods. (*—The asterisk is used to indicate anomalies.)

Samples	LREE															HREE					Total Σ REE	Ratio LREE/ HREE	Normalized Values To NASC						Texture			Chemical Condition	
	La	Ce	Pr	Nd	Sm	Eu	Gd	Dy	Ho	Er	Yb	Lu	Y	Sc	Hf	(La/Yb) _N	(La/Sm) _N	(La/Gd) _N	(Gd/Yb) _N	Eu/Eu*			Ce/Ce*	Sand	Silt	Clay	pH	Eh					
	(μgg ⁻¹)															HREE							(%)	(%)	(%)	(mV)							
Sabana Yegua: Rainy Season																																	
SY2	10.376	25.894	3.057	14.245	3.190	0.874	3.430	3.451	0.517	2.504	1.817	0.375	18.518	27.996	1.925	69.730	4.765	0.553	0.579	0.492	1.125	1.160	1.001	0.05	43.73	56.22	6.74	-41					
SY3	10.915	27.764	3.372	14.486	3.306	0.888	3.428	3.466	0.511	2.404	1.834	0.372	18.661	26.121	2.140	72.747	5.054	0.577	0.588	0.517	1.114	1.158	0.997	0.03	47.36	52.61	6.75	-57					
SY9	13.522	30.987	3.696	15.622	3.356	0.907	3.290	3.300	0.470	2.285	1.698	0.362	16.465	21.784	1.232	79.495	5.970	0.772	0.718	0.668	1.155	1.198	0.955	0.70	59.62	39.67	6.85	9					
SY10	10.489	29.363	3.641	16.507	3.874	1.022	4.036	3.836	0.603	2.448	1.979	0.389	20.393	26.067	2.586	78.188	4.882	0.513	0.482	0.422	1.216	1.135	1.035	14.89	62.88	22.23	6.79	-50					
SY11A	0.907	27.552	3.142	14.862	3.624	1.038	3.882	3.634	0.561	2.143	1.843	0.378	19.102	29.619	3.120	71.756	4.768	0.478	0.447	0.381	1.256	1.215	1.122	5.57	52.06	42.36	6.75	-65					
SY13	11.483	25.047	2.850	12.792	3.225	0.897	3.455	3.566	0.531	2.334	1.839	0.383	18.715	29.279	2.150	68.402	4.649	0.605	0.634	0.540	1.120	1.180	0.954	7.60	22.33	70.07	6.71	-62					
SY14	15.418	27.489	3.123	13.175	3.024	0.817	2.802	3.012	0.399	2.146	1.365	0.338	13.814	16.090	2.056	73.108	6.266	1.095	0.908	0.894	1.224	1.233	0.863	54.52	19.77	25.70	7.26	-50					
Maximum	15.418	30.987	3.696	16.507	3.874	1.038	4.036	3.836	0.603	2.504	1.979	0.389	20.393	29.619	3.120	79.495	6.266	1.095	0.908	0.894	1.256	1.233	1.122	54.52	62.88	70.07	7.26	9					
Minimum	0.907	25.047	2.850	12.792	3.024	0.817	2.802	3.012	0.399	2.143	1.365	0.338	13.814	16.090	2.132	68.402	4.649	0.478	0.447	0.381	1.114	1.135	0.863	0.03	19.77	22.23	6.71	-65					
Average	11.614	27.728	3.269	14.527	3.371	0.920	3.475	3.467	0.513	2.323	1.768	0.371	17.953	25.280	2.173	73.347	5.194	0.656	0.622	0.559	1.173	1.182	0.990	11.91	43.97	44.12	6.84	-45					
Median	10.915	27.552	3.142	14.486	3.306	0.897	3.430	3.466	0.517	2.334	1.834	0.375	18.661	26.121	2.140	72.747	4.882	0.577	0.588	0.517	1.155	1.180	0.997	5.57	47.36	42.36	6.75	-50					
SD	1.991	1.849	0.290	1.204	0.266	0.074	0.373	0.242	0.060	0.131	0.181	0.015	2.001	4.475	0.539	3.812	0.601	0.199	0.144	0.161	0.054	0.032	0.074	18.09	15.74	15.74	0.18	23					
CV (%)	17.144	6.669	8.874	8.290	7.895	8.077	10.730	6.973	11.764	5.644	10.245	4.176	11.144	17.703	24.789	5.197	11.575	30.330	23.066	28.784	4.581	2.714	7.493	151.90	35.79	35.66	2.61	-52					
Sabana Yegua: Dry Season																																	
SY1	12.007	31.125	2.359	15.921	3.111	0.979	3.368	5.609	0.688	1.880	2.054	0.271	20.230	25.079	2.582	79.373	4.723	0.566	0.687	0.579	0.977	1.328	1.274	0.66	33.49	65.86	6.68	-94					
SY3	12.292	31.433	2.621	15.748	3.175	0.987	3.373	5.628	0.695	2.037	2.046	0.267	20.075	25.094	2.504	80.301	4.717	0.582	0.690	0.592	0.983	1.324	1.206	1.20	29.94	68.86	6.85	-80					
SY4	12.834	31.766	2.492	15.009	2.847	0.922	2.951	5.422	0.584	1.839	1.722	0.224	17.335	20.921	2.711	78.610	5.170	0.722	0.803	0.707	1.022	1.396	1.224	12.36	29.71	57.93	6.81	-87					
SY5	12.282	32.061	2.379	16.711	3.361	1.064	3.644	5.705	0.749	1.810	2.185	0.295	21.541	28.330	3.173	82.245	4.716	0.545	0.651	0.548	0.994	1.335	1.292	0.47	40.21	59.32	6.85	-104					
SY6	13.505	31.826	3.064	15.740	3.193	0.937	3.168	5.599	0.647	2.152	1.932	0.250	18.807	18.475	2.227	81.970	4.980	0.677	0.753	0.693	0.978	1.293	1.078	0.40	55.96	43.65	6.65	-94					
SY7A	9.447	28.824	1.926	14.019	2.878	0.978	3.353	5.619	0.686	2.132	2.004	0.255	19.789	27.468	2.246	72.120	4.134	0.457	0.585	0.458	0.997	1.383	1.472	8.48	30.85	60.67	6.94	-104					
SY8A	9.148	28.399	1.896	13.667	2.899	0.965	3.231	5.604	0.678	2.042	1.952	0.249	19.281	26.723	2.135	70.729	4.142	0.454	0.562	0.460	0.987	1.384	1.485	1.41	63.72	34.87	7.87	-106					
SY9A	11.873	31.762	2.805	15.871	3.440	1.060	3.595	5.715	0.733	2.045	2.085	0.268	20.663	25.027	2.264	81.254	4.626	0.552	0.615	0.537	1.028	1.324	1.199	2.09	37.18	60.73	6.84	-121					
SY10	13.771	35.077	3.499	17.746	3.657	1.160	3.720	5.706	0.727	2.070	1.996	0.256	19.693	20.861	2.929	89.384	5.175	0.668	0.671	0.602	1.111	1.381	1.101	66.94	17.40	15.66	7.06	-109					
SY13	14.206	13.338	4.412	17.359	3.968	1.101	3.619	3.648	0.750	2.135	1.920	0.326	21.245	28.841	2.682	66.784	4.386	0.717	0.638	0.638	1.124	1.276	0.367	0.75	25.13	74.12	6.68	-92					
SY14	15.560	17.293	4.247	17.740	3.696	0.966	3.151	3.091	0.636	1.942	1.685	0.289	18.437	19.762	2.610	70.296	5.513	0.895	0.750	0.803	1.115	1.243	0.463	9.92	34.21	55.87	6.68	-106					
SY15	12.206	14.633	3.525	15.358	3.657	1.017	3.230	3.271	0.666	2.067	1.680	0.280	18.694	26.191	2.736	61.588	4.503	0.704	0.595	0.614	1.147	1.299	0.486	35.16	34.13	30.72	6.80	-116					
Maximum	15.560	35.077	4.412	17.746	3.968	1.160	3.720	5.715	0.750	2.152	2.185	0.326	21.541	28.841	3.173	89.384	5.513	0.895	0.803	0.803	1.147	1.396	1.485	66.94	63.72	74.12	7.87	-80					
Minimum	9.148	13.338	1.896	13.667	2.847	0.922	2.951	3.091	0.584	1.810	1.680	0.224	17.335	18.475	2.135	61.588	4.134	0.454	0.562	0.458	0.977	1.243	0.367	0.40	17.40	15.66	6.65	-121					
Average	12.428	27.295	2.935	15.907	3.323	1.011	3.367	5.048	0.687	2.013	1.938	0.269	19.649	24.398	2.567	76.221	4.732	0.628	0.667	0.602	1.039	1.331	1.054	11.65	35.99	52.35	6.89	-101					
Median	12.287	31.279	2.713	15.809	3.277	0.983	3.360	5.606	0.687	2.043	1.974	0.267	19.741	25.087	2.596	78.992	4.717	0.625	0.661	0.597	1.010	1.326	1.202	1.75	33.81	58.62	6.83	-104					
SD	1.740	7.270	0.798	1.266	0.351	0.068	0.226	0.998	0.047	0.112	0.156	0.025	1.164	3.364	0.298	7.558	0.403	0.121	0.071	0.096	0.063	0.046	0.375	19.19	12.13	16.72	0.32	11					
CV (%)	14.000	26.636	27.178	7.960	10.572	6.757	6.717	19.764	6.909	5.581	8.071	9.316	5.926	13.787	11.604	9.916	8.519	19.282	10.662	15.862	6.046	3.475	35.557	164.69	33.70	31.94	4.59	-11					

Apart from a high spatial uniformity in each reservoir, the chemistry of REE in the sediments is also uniform between the two systems, reflecting a high homogeneity of sedimentation and similarity of climatic conditions and morphometric and chemical characteristics of the lakes and lithological sources, although they are more diverse in Sabana Yegua.

4.2.1. Geochemical Behavior of Rare Earth Elements in the Bottom Sediments

The sediments have total contents of REE between a narrow range of 61.6–89.4 μgg^{-1} in Sabana Yegua and 58.2–96.2 μgg^{-1} in Tavera, with coefficients of variation (CV) of 9.9% and 14.3%, respectively (Table 5). The low CV are confirmed for all elements, indicating a homogeneous spatial distribution. In both reservoirs, the elements with a more heterogeneous distribution (CV: 20–40%) correspond to those whose contents reflect the local redox conditions and are strongly influenced by postpositional modifications, such as Ce, and to those with more diverse sources, such as Pr, Dy, and Hf.

Ce, Nd, and La are the most abundant elements, accounting for 70–75% of the ΣREE . Values normalized to NASC, which are always less than 1 for all lanthanides, Y, and Hf, indicate the occurrence of impoverished sources of these elements in the drainage areas. The exception is Sc, with normalized values of 1.7 in Sabana Yegua and 2.3 in Tavera, indicating significant enrichment of this element. The higher levels of this element could be explained by its preferential sorption by clay minerals and organic compounds [50], key constituents of the sediments [26,27].

Looking at the average values of the continental crust and a reference sediment [7], and comparing the normalized REE distribution patterns (Figure 4), most sediments show a clear depletion of LREE (La–Nd), similar values for MREE and HREE, with only a slight enrichment for Eu, Dy, and Lu, and a notorious enrichment for Sc. The REE distribution in the sediments gives normalized patterns with weak fractionation and homogeneous values of the LREE/HREE ratio in both reservoirs and between seasons (see Table 5). This ratio is lower than the values established by [53] for an average sediment (9.79) and for the upper continental crust (9.7): in sediments, the high homogeneity of the REE distribution and the depletion of LREE compared to the upper crust is also reflected in the uniform values of the fractioning parameters $(\text{La}/\text{Yb})_{\text{N}}$, $(\text{La}/\text{Sm})_{\text{N}}$, and $(\text{La}/\text{Gd})_{\text{N}}$ (between 0.394 and 0.686, CV < 20% in Tavera, and between 0.517 and 0.661, CV < 30% in Sabana Yegua).

While Eu anomalies are always positive and uniform (median values of 1.2 in both reservoirs, CV: 0.47–3.48%), Ce anomaly is the parameter that shows the greatest variability along the reservoirs and between the two sampling periods. The variations observed in the Ce anomalies indicate the differentiation between Ce and the other REE during the processes of transport and deposition of the sediments. The Eu anomalies are generally inherited from the source rocks, which explains their uniformity between the two reservoirs and during the year.

Considering the distribution of Ce and Eu in both systems, there does not seem to be a significant relationship between their contents and anomalies related to sediment pH or redox conditions of the sediments, as reported by several authors [18,23]. The absence of this relationship can be seen in the low correlation factors ($r < 0.2$) and in the distribution of Ce anomalies in Sabana Yegua. In this reservoir, the negative Ce/Ce* values in the sediments under the influence of detrital and carbonate rocks in Las Cuevas River basin (with Ce/Ce* between 0.142 and 0.213, according to [25,26]), clearly show the influence of these rocks on the concentration of this element, while in the other sectors of the reservoir, the values vary between 1.101 and 1.480 under similar reducing conditions. The Eu anomaly is more evenly distributed over the reservoir, with values ranging from 0.153 to 0.201 and CV of 7.33%.

Unlike several authors [7,54,55] who suggest that the total contents of REE lie in trace minerals (zircon, monazite, apatite, etc.) concentrated preferentially in the finest fractions (silt and clay), the particle size does not seem to have a significant influence on the REE values of the sediments of both reservoirs. The highest correlation values, although

with low significance (r between 0.4 and 0.5), were observed for the silty fraction, which, similarly to the soils of the basins, shows the importance of this fraction for the storage of these elements. The low correlation may be explained by the high textural homogeneity of the sediments (see data in Table 5). As in other similar studies [56–59], the ratio between LREE/HREE in sediments, the Ce and Eu anomalies, and the fractionation parameters are not related to texture, either.

4.2.2. Seasonal Variability of the Rare Earth Elements in the Reservoir Sediments

The seasonal variability of REE is not the same for both reservoirs, or for all elements. Apart from the fact that REE may have different sources, the variations observed between seasons, even if small, may be due to the mixing of different waters, which may change the pH and salinity of the lakes, as well as to seasonal changes in redox conditions, adsorption–desorption reactions, and REE complexation, as observed by [21].

In each reservoir, there is a high uniformity in the distribution of REE, between the two sampling periods, with coefficients of variation of less than 10% and a negligible increase in the drier period: (1) in Sabana Yegua, the small increase (ΣREE : 72.75 \rightarrow 78.99 μgg^{-1}) is due to a slight enrichment of La, Ce, Nd, Dy, Ho, Yb, Y, and Hf, accompanied by a slight decrease of Pr, Er, and Lu. The uniform seasonal variation of elements by the two main groups of REE leads to uniformity of the LREE/HREE ratio; (2) in Tavera, some differences are observed regarding the seasonal changes of these elements. The higher values in the drier season (ΣREE : 71.84 \rightarrow 76.57 μgg^{-1}) are due to the balance between the increase of some LREE, such as La, Pr, Nd, and Sm, and the decrease of elements from the MREE and HREE groups (Gd, Dy, Ho, Er, Yb, and Lu), leading to an increase of the LREE/HREE ratio. In both reservoirs, enrichment of La in the drier season enhances the LREE fractionation relative to MREE and HREE, as measured by higher ratios of $(\text{La}/\text{Yb})_{\text{N}}$, $(\text{La}/\text{Sm})_{\text{N}}$, and $(\text{La}/\text{Gd})_{\text{N}}$.

There are some processes that may explain the slight increase in the total content of REE in the dry season, often followed by a marked increase in the light elements (LREE):

- (1) Light elements (LREE) are preferentially scavenged on the surface of particles of Fe–Mn oxides and of clay minerals, transported in suspension during the rainiest periods, and may also be precipitated as REE phosphates. HREE usually form dissolved complexes that remain in solution [56,58]. The pH values of the water column, which are always higher than those of the sediments (with median values of 6.8–6.9), are slightly alkaline with values between 7.5 and 9 [27]. The pH is slightly higher during the dry season, which is associated with an increase of salinity. According to [23], these pH values favor the release of REE from the surface of the fine-grained suspended particles, so that these elements are removed by the water and enrich the bottom sediments.
- (2) At this season there is also a greater tendency to flocculation, followed by the precipitation of particles in suspension.
- (3) Increase in the rate of decomposition of organic compounds, followed by the release of REE and subsequent deposition in sediments [18,19]. This process was clearly observed in Tavera, where the higher levels of organic compounds were found [26,27]. In this reservoir, with the exception of the lighter elements (La, Ce), there is a marked increase in the contents of most of the rare elements in a sector near the mouth of the Yaque del Norte, the sediments of which were covered in the driest period by a thin film of water rich in organic debris. This reservoir also has the greatest dispersion of Ce content (CV of 41.5%), the rare element most dependent on local redox conditions. The decomposition reactions of organic material can lead to changes in oxidation–reduction conditions, increasing the variation in Ce content.
- (4) Between the two seasons and along the reservoirs, the Ce anomaly is the parameter that shows the greatest variability, indicating the differentiation between Ce and the other REE during the processes of transport and deposition of the sediments. This variability is due to the easy fractionation by oxidation of Ce^{3+} to Ce^{4+} . Some of the variation observed in Ce anomalies between seasons and between reservoirs

could possibly be a consequence of (1) changes in dissociation rates of Ce-rich humic complexes under more alkaline conditions [9], (2) removal of Ce-rich organic complexes present in the water column, under more reductive conditions and in the presence of components with strong adsorption capacities [9,19], or (3) changes in the behavior of complexation and adsorption of REE by organic complexes, clay minerals, or Fe–Mn-oxides, with subsequent changes in the oxidation states of Ce^{3+} – Ce^{4+} [18], which can be separated as insoluble oxyhydroxides [9,18].

4.2.3. Relationship between the Distribution of Rare Earth Elements in Sediments and in Soils of Drainage Areas

The low coefficients of variation of the sediments contrast with the great heterogeneity of REE distribution in the basins' soils, with CV of 31.5% in the Tavera basin and 21.7% in Sabana Yegua's. In both reservoirs, in addition to a higher homogeneity of values, there is a significant increase in the total contents of REE in relation to the soils, which could be related to the increase of silty-clay components in the sediments due to the selective erosion of the finer particles of the soils, where these elements are preferentially retained. The slightly alkaline pH of the reservoir water (pH 7.5–9.0) may also increase the accumulation in REE, since according to [23], these pH values favor the release of these elements from the surface of the Fe and Mg oxides and clay particles transported in suspension, which can subsequently be bound by the soil sediments.

Comparing the LREE/HREE ratio, LREE enrichment, albeit minor, is evident in the sediments of both reservoirs. This enrichment is confirmed by the increase in the contents of La, Ce, Pr, and Nd and by higher fractionation parameters $(La/Yb)_N$, $(La/Sm)_N$, and $(La/Gd)_N$. From soils to sediments, the invariability of the fractionation parameter $(Gd/Yb)_N$, which reflects the MREE/HREE ratio, indicates the stability of the elements from the series (Sm–Ho) through the geological processes involved in erosion and transport of soil particles to the lake bottom. The values of the elements accompanying lanthanides (Y, Sc, and Hf) are also invariant.

The Ce anomalies, although corresponding to an important indicator of redox status [19], are much more uniform than those of the basin bottoms, emphasizing the homogeneity of sedimentation and physical and chemical conditions of these lacustrine environments. Compared to the source soils, Ce anomalies decrease in the sediments of both reservoirs, indicating the highly reducing conditions of the soil, which contrast strongly with the oxidizing conditions of the soils. The surface sediments of Sabana Yegua and Tavera reservoirs consistently exhibit negative redox potential values, with Eh ranging from -94 mV to -121 mV and -65 mV to -97 mV, respectively, in the driest period, and from $+9$ mV to -65 mV and -2 mV and -48 mV in the wet season. These conditions cause the reduction of the particulate form of Ce (Ce^{4+}) to a more soluble form (Ce^{3+}), which is released into the water column, resulting in a depletion of Ce in the sediments, compared to the neighboring element pairs La and Pr.

Eu behaves differently to Ce because there is a close relationship of Eu with the nature of the source material in the basins [11] and it is less sensitive to redox conditions of the environment than Ce. In relation to soils, Eu anomalies are invariable in Sabana Yegua and there is a slight decrease in the sediments of Tavera. This decrease may be associated with the depletion of this element during the processes of oxidation and mobilization of Eu from soils by conversion.

Eu behaves differently from Ce because there is a close relationship between Eu and the nature of the parent material in the basins [11] and it is less sensitive to ambient redox conditions than Ce. With respect to soils, Eu anomalies are invariable in Sabana Yegua, and a slight decrease is observed in Tavera sediments. This decrease could be related to the depletion of this element during the oxidation processes and the mobilization of Eu from the soils through the conversion of Eu^{2+} to Eu^{3+} , a more mobile form that could have been transported in solution to the water column. The nondependence of this element on the strongly reducing conditions at the bottom of the reservoirs suggests that the redox

conditions in the sediments or at the sediment–water interface are not sufficient to alter the oxidation state of Eu, as observed in other lakes by [18].

4.2.4. Rare Earth Elements Analysis as a Potential Proxy of Sediments Provenance

In lacustrine sediments, which are usually silty-clayey and rich in organic matter, the finer particles act as a pool for REE. The marked increase in the total content of REE and the slight enrichment of LREE in the sediments, compared to the soils of the catchments, could be a consequence of the predominance of secondary minerals in the sediments, such as phyllosilicates, Fe- and Al-oxides, and hydroxides, in which these elements are normally retained by adsorption reactions. In these sedimentary materials, with pH of about 6–7, the degree of retention is high, and inner sphere complexes are formed [15].

The low ratio between the area of the lakes and the area of the catchments and the tropical climate with its high annual rainfall, two of the main factors responsible for the homogeneity of the distribution patterns of REE, did not allow the specific contribution of the different rock or soil groups to be determined for each sector of the reservoirs. An exception is the sector in Sabana Yegua located in the alluvial fan of the Las Cuevas River, which has similar values to those of the basin rocks, limestones, and detrital rocks with carbonate nature, indicating the inheritance of the REE patterns.

1. Despite the great uniformity of the REE distribution patterns in the reservoirs, slight differences in the concentration of some elements are discernible between the two, Which could be related to the greater or lesser contributions of the different lithotypes of the basins or, to a lesser extent, to changes in the redox conditions of the environment (mainly for Ce):
 - Of the lighter (LREE) and heavier (HREE) elements, La and Nd in the first group and Ho, Yb, and Lu in the second group have identical concentrations in both reservoirs, suggesting that they originate from similar lithologies in the basins.
 - Elements such as Pr, Sm, Eu, Gd, and Er, which have highest concentrations in tonalites, granites, granodiorites, and schists [50], slightly increase in Tavera, whose basin is very representative of those lithologies [25–27]. The lowest concentration of these elements is found in carbonate rocks, which have a strong influence on the sedimentation of Sabana Yegua, where the lowest concentrations of these elements are found.
 - Dy behaves irregularly because, although the highest values have been found in ultramafic, mafic, and intermediate rocks of Tavera basin [25–27], the sediments of Sabana Yegua have the highest, and more uniform, concentrations of this element, except in the sediments under the influence of carbonate rocks.
 - According to the data obtained for the chemistry of REE in the rocks of the basins [25–27], Ce has the highest concentrations in the basic and intermediate rocks of the Sabana Yegua basin, confirming the slightly higher values in the sediments deposited in this reservoir.
- In the Sabana Yegua reservoir, the spatial distribution of the different elements illustrates the greater uniformity of their concentration and the specific sedimentation conditions of the sector under the influence of the carbonate rocks of the Las Cuevas River sub-basin (Figure 5). The small variations in the distribution of REE with CV of 10%, in the absence of significant textural differences in sediments and redox conditions, may be related to the greater or lesser contribution of the different lithotypes that outcrop in the three sub-basins:
 - A slight depletion of the total contents of REE (except Sc) is observed in the NE sector of the lake, under the influence of an extensive area of coarse detrital rocks (conglomerates and sandstones) and igneous and volcanic sedimentary rocks in the Grande del Medio River basin.

- The highest Σ REE values in the sediments, except for some elements of the MREE group (Ho, Dy), are found in the sector of the lake under the influence of the Yaque del Sur River, which appears to be the sub-basin responsible for the largest supply of REE in this system. These higher concentrations extend throughout the W sector of the lake to the dam wall, where the greatest depths are found, indicating a preferential N–S direction of the circulation of sediments from this sub-basin.
- The distribution of REE in the SE sector of the reservoir, influenced by carbonate and detrital rocks from the Las Cuevas River, shows a slight depletion of the sum of REE, higher contents of lighter elements (La, Pr, and Nd) and lower contents of Dy, Yb, and Sc, leading to an increase in the fraction parameters of light–middle and light–heavy REE (represented by higher ratios $(La/Yb)_N$, $(La/Sm)_N$, and $(La/Gd)_N$). This sector also shows lower anomalies of Ce and Eu. These distribution patterns correspond to those of the carbonate rocks (see Table 3), indicating strong inheritance from these sedimentary rocks.
- The spatial distribution of the total contents of REE along Tavera Reservoir (Figure 6) shows a decreasing gradient from the confluence of the Yaque del Norte River, where the highest values were found, to the dam. These values are generally higher in the southern shoreline area of the lake, where the particulate load from this river preferentially circulates and appears to be the area that also receives a high sediment load from the watershed runoff.

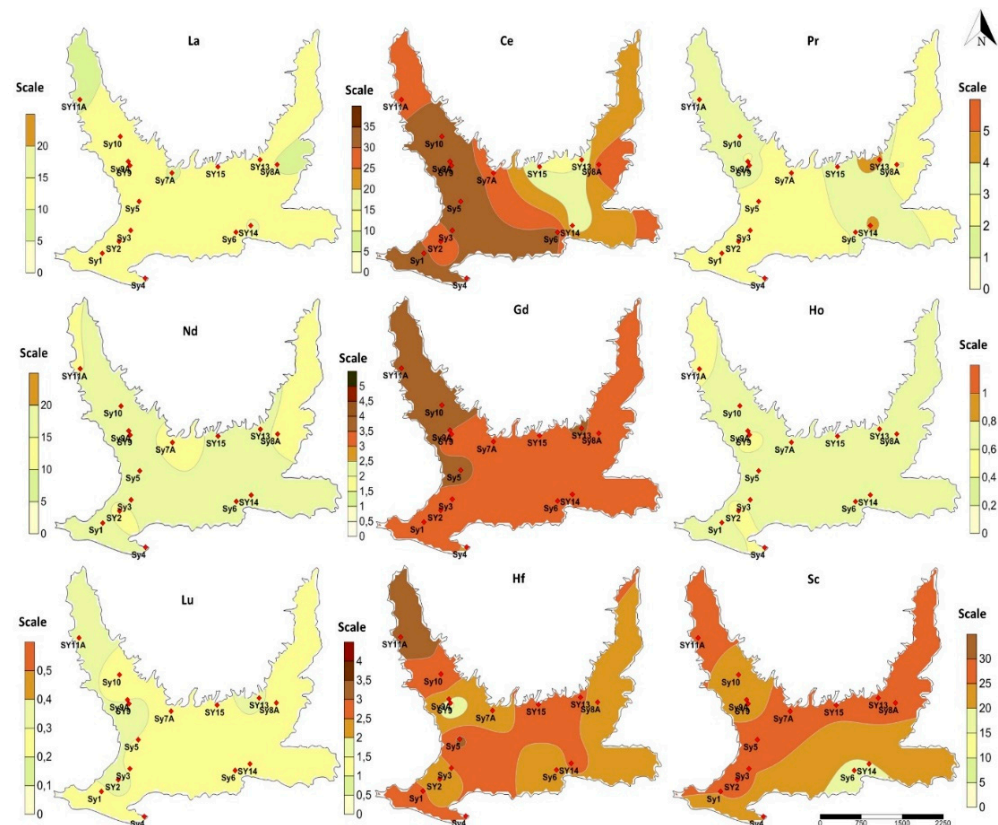


Figure 5. Maps of the REE distribution in surface sediments of Sabana Yegua reservoir (in $\mu\text{g g}^{-1}$). Only the most representative elements are depicted as an example.

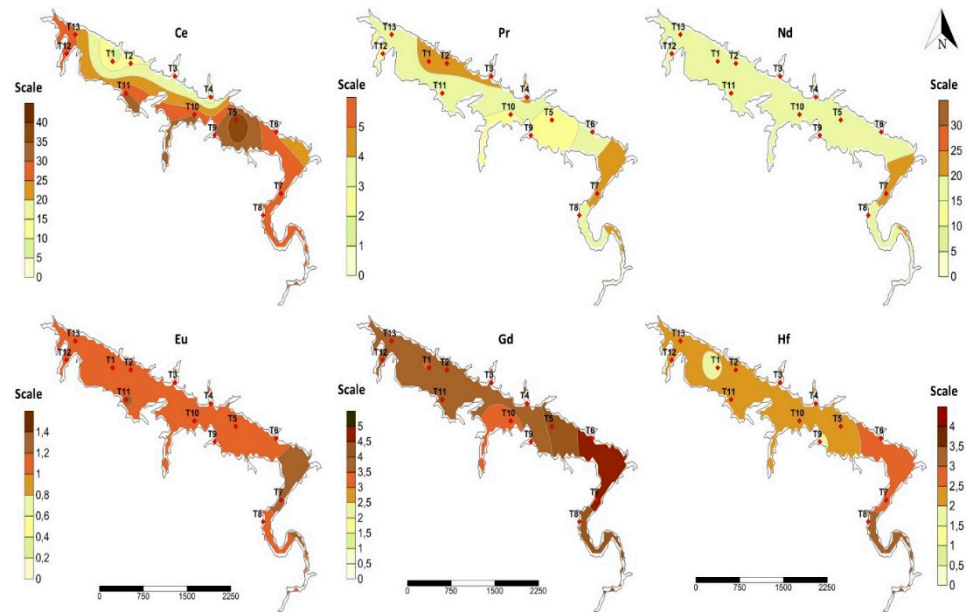


Figure 6. Maps of the REE distribution in surface sediments of Tavera reservoir (in $\mu\text{g g}^{-1}$). Only the most representative elements are depicted as an example.

This graded distribution is followed by most elements. Except for the lighter elements La and Ce, the higher values are located at the mouth of the only tributary of this lake, although some elements, such as Pr, Sm, Er, and Y, also have high point concentrations near the northern edge of the reservoir, close to the dam wall. As observed by several authors [50], Pr and Sm show similar spatial distribution.

2. Considering the bivariate plots used as indicators to determine the sources of the sediments (Figure 7), the $\sum\text{REE}$ vs. LREE/HREE data of the sediments were plotted to reflect the fractionation of REE and its relationship to the patterns of different groups of soils and rocks from the basins (Figure 7A,B). In both time periods, the LREE/HREE ratio in the sediments ranges from 4.13–6.27 in Sabana Yegua and 3.77–6.16 in Tavera. These sediment data are consistent with the average values determined: (1) in Sabana Yegua with soils in low-relief topography, soils derived from Quaternary deposits in the Yaque del Sur basin (SYS3) and soils derived from detrital and carbonate rocks in the Las Cuevas basin (SYS8, SYS9); (2) in Tavera with soils in low-relief topography of the W tributary of the Yaque del Norte River (TS3, TS5) derived from tonalites. In the bivariate diagrams, these soils correspond to points bounded by the ellipse.

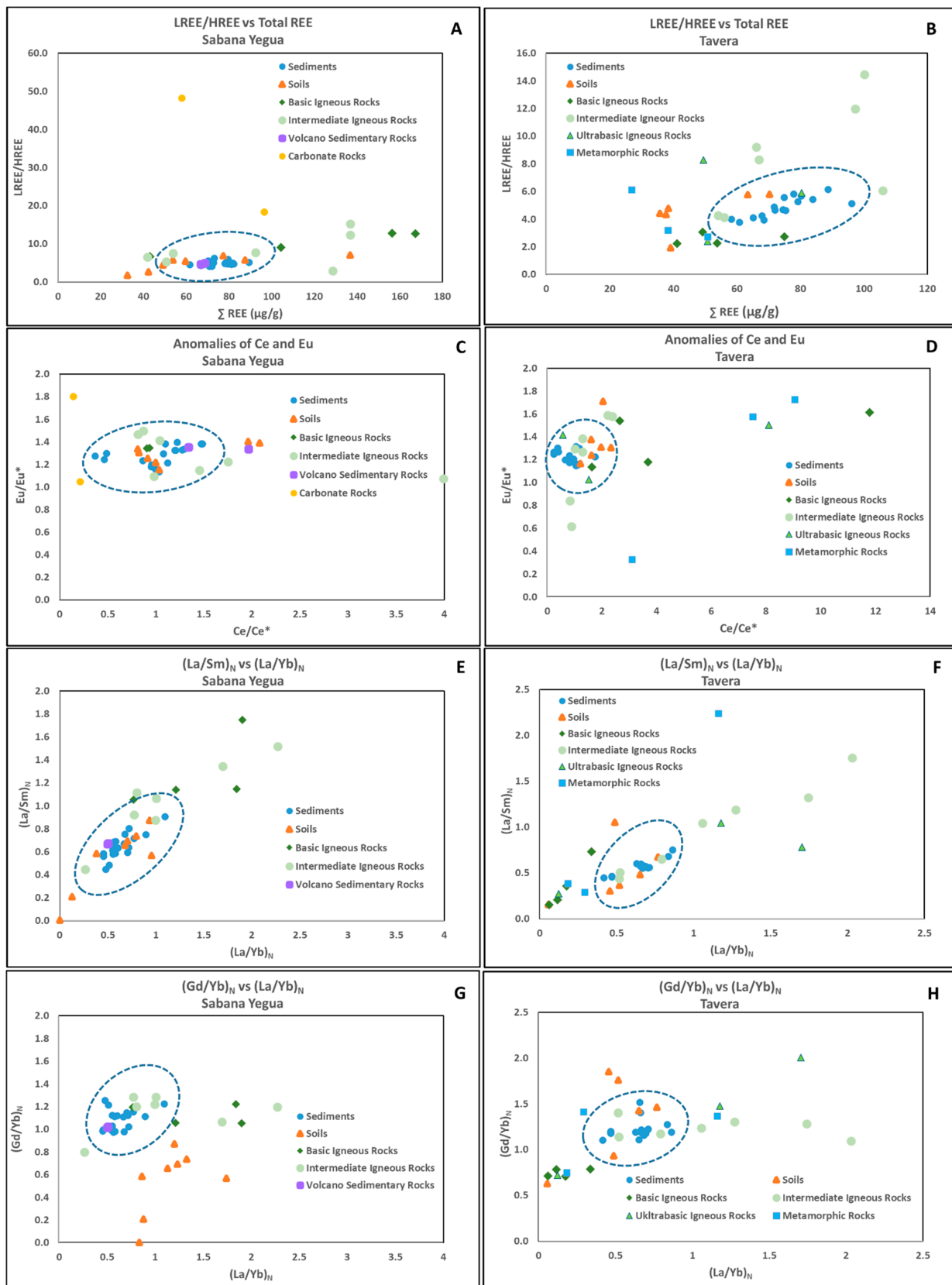


Figure 7. Bivariate plots of Σ REE and LREE/HREE (A,B), Eu and Ce anomalies (C,D), and representative fractionation parameters of light and heavy rare earth elements: $(\text{La}/\text{Sm})_N$ vs $(\text{La}/\text{Yb})_N$ (E,F) and $(\text{Gd}/\text{Yb})_N$ vs $(\text{La}/\text{Yb})_N$ (G,H) for sediments, soils, and rocks from Sabana Yegua and Tavera basins.

With respect to the rocks of the basins, the LREE/HREE values for the sediments and their projection in the diagrams are close to the values found in (1) Sabana Yegua: volcano-sedimentary rocks (2-S1, 2-S1A, 2-S3) in steeply sloping areas of the Rio Grande del Medio basin; intermediate igneous rocks (2-S9, 2-S8), and basaltic rocks (2-S6), both groups in areas with lower slopes of the Yaque del Sur basin; (2) Tavera: intermediate igneous rocks with tonalitic and granodioritic compositions (2-T9, 2-T9A), and ultramafic igneous rocks near the main inflow of the reservoir (2-T8), both groups in low-relief topography.

3. To obtain a better overview of the potential sources of sediments, Ce/Eu anomalies and the ratio of normalized contents of some key elements, $(La/Yb)_N$, $(La/Sm)_N$, $(La/Gd)_N$, and $(Gd/Yb)_N$, were also recorded for the different groups of rocks, soils, and sediments.

- Bivariate plots for Eu and Ce anomalies show an overlap of data in the Sabana Yegua sediment projection (Figure 7C) with the same rock and soil groups observed in the Σ REE vs. LREE/HREE projection, including a greater number of soils as likely sources. Sediments have average values of Eu/Eu^* similar to the volcano-sedimentary rocks of the Rio Grande del Medio basin and to the average values of intermediate igneous rocks at the margins of the Yaque del Sur River. Ce/Ce^* in sediments deposited in the alluvial fan of Las Cuevas River show a more heterogeneous distribution and negative anomalies ($Ce/Ce^* = 0.367\text{--}0.486$), which are clearly inherited from the carbonate rocks of the watershed ($Ce/Ce^* = 0.142\text{--}0.213$). At Tavera, the influence on the Ce and Eu anomalies of sediments includes the same river margin soils in the western sector of the basin (TS3, TS5, TS1) derived from tonalitic and volcano-sedimentary rocks (Figure 7D). In addition to the influence of intermediate and basic igneous rocks located in low-relief topography of the western branch of Yaque del Norte (2-T7, 2-T8), various lithologies (tonalites, gabbros, ultramafic rocks) from higher elevations in the two sub-basins (1-T2, 1-T3, 2-T4, 2-T14) also contribute. Since the anomalies of these two elements (especially Ce) can be affected by the redox conditions of the surrounding environment, there is a wider dispersion of the likely sources of the accumulated sediments; this is one of the main reasons why only the common soils and rocks associated with the sediments should be considered in all bivariate diagrams.
- The diagrams corresponding to the fractionation parameters of light and heavy REE: $(La/Sm)_N$ vs. $(La/Yb)_N$, $(Gd/Yb)_N$ vs. $(La/Yb)_N$, $(La/Yb)_N$ vs. Yb_N , $(La/Sm)_N$ vs. Sm_N , and $(La/Yb)_N$ vs. Ce_N (Figure 7E–H), show, in both systems, in addition to the soil and rock sources obtained from the Σ REE vs. LREE/HREE correlation plots, the influence of soils and rocks from sectors farther from the lakes and with steeper slopes: (1) in Sabana Yegua, sediment fractionation parameters correlate with those of a soil composed of detrital rocks (SYS10) and intermediate igneous rocks (2-S2, 2-S3) in the higher and steeper areas of the Las Cuevas basin; (2) in Tavera, the data of a tonalitic rock (2-T13) and a tonalitic soil (TS6, TS7) in areas with steep slopes, in the extreme SE and in the western tributary of the Yaque del Norte, overlap on the sediments projection.

In summary, by the similarity of the ratios between the fractionation parameters of light and heavy REE and the anomalies of Ce and Eu, and by the superposition on the sediment projection in bivariate diagrams, it is possible to infer, in a first approximation, the areas of higher influence on the sedimentation of both reservoirs, delineated on the maps in Figure 8.

- (1) Sabana Yegua reservoir—sediments deposited in the alluvial fan of the Las Cuevas River in the sector SE are mainly fed by soils in the shallowest topography developed on detrital and carbonate rocks (area S1), and by intermediate igneous rocks located in the areas of greater slope in the area NE of this sub-basin (area R1). Sedimentation

- in the other sectors of the lake is influenced by (i) soils derived from Quaternary deposits on the margins of the Yaque del Sur (area S2), (ii) volcano-sedimentary rocks in steeply sloping areas in the Rio Grande del Medio watershed (area R2), and (iii) rocks of different nature in a mountainous area in the central region of the Yaque del Sur watershed (intermediate igneous and basaltic rocks (area R3)). Although the volcano-sedimentary rocks of the Rio Grande del Medio basin are one of the main sources of sediment, there is no significant relationship with the soils of this basin, probably because they are undeveloped soils in areas with steep slopes. The distribution of the highest Σ REE values in the NW sector of the lake indicates that the Yaque del Sur River should be the tributary responsible for the largest influx of REE.
- (2) Tavera reservoir—with only one tributary, the Yaque del Norte River, sediments have contributions of soils and rocks distributed in two sub-basins of this river. Soils with greater influence are in two distinct areas of the watershed: (i) soils composed of tonalites influenced by volcano-sedimentary rocks in the low-lying topography of the eastern tributary (area ST1), and (ii) tonalite soils in the steep slopes of the western tributary (area ST2). Rocks that could correspond to the main sources of sediments are also scattered in the two sub-basins: (i) intermediate igneous rocks of tonalitic and granodioritic composition in a flattened area near the reservoir (area RT1), (ii) ultramafic igneous rocks in the western tributary (area RT2), and (iii) tonalitic rocks in an area of steep slopes at the SE boundary of the eastern tributary (area RT3).

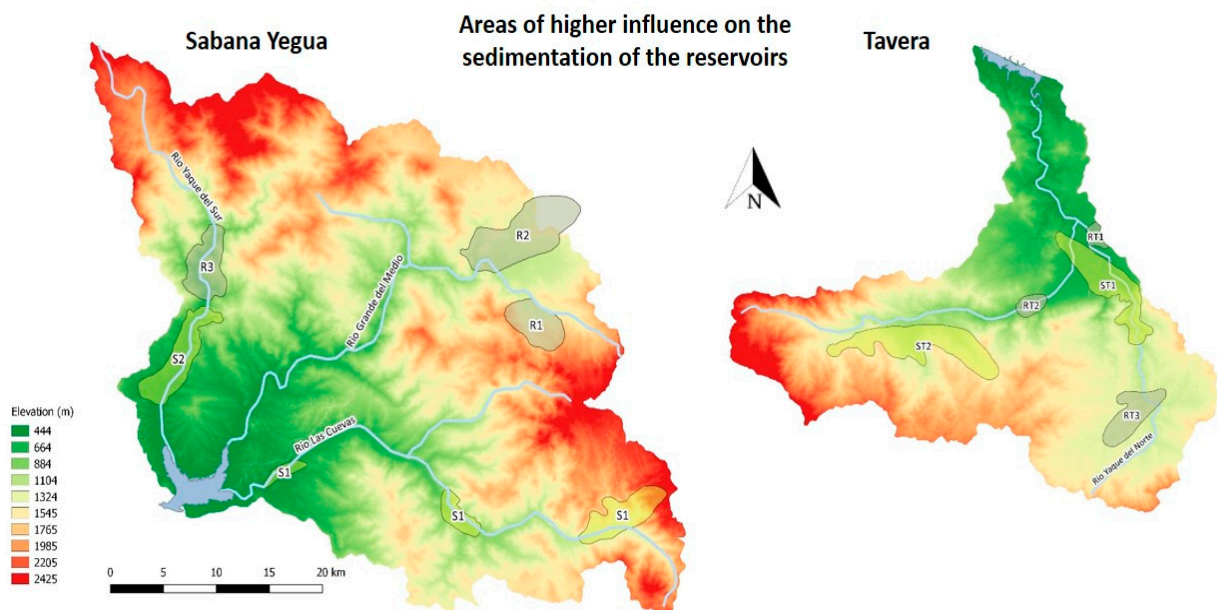


Figure 8. Areas of higher influence on the sedimentation of the reservoirs: S—soils (Sabana Yegua basin), ST—soils (Tavera basin), R—rocks (Sabana Yegua basin), RT—rocks (Tavera basin).

5. Conclusions

This study is based on the analysis of a very complex and important group of elements—rare earth elements (REE)—in the sediments accumulated in two dam reservoirs in the Dominican Republic (Sabana Yegua and Tavera), with two main objectives: (1) to understand the spatial and seasonal behavior of these elements in tropical systems regularly exposed to extreme climatic events, and (2) to define, as a potential proxy, the areas of higher influence on sedimentation of both reservoirs.

The main conclusions can be summarized as follows:

1. The spatial distribution of REE in the sediments of the reservoirs shows a high spatial uniformity in both systems and between them, reflecting a high homogeneity of sedimentation and similarity of (i) climatic conditions, (ii) lithological sources,

- (iii) morphometric and chemical characteristics of the lakes, and (iv) nature of sediments, mostly clayey and silty. This homogeneity can be slightly reduced by some mechanisms of REE mixing and removal within these systems, such as (i) mixing of detrital fractions from weathering of different sources, (ii) removal of dissolved REE in the water column by suspended or bottom sediments, (iii) planktonic removal, (iv) co-precipitation of REE with iron hydroxides, (v) presence of sediments with higher sand content, which have a dilution effect on the concentration of these elements, (vi) runoff effects from the banks, (vii) groundwater discharge, which can affect the salinity of the water column, and (viii) aggregation of colloidal particles transported in suspension into these systems induced by increased salinity during periods of lower precipitation, according to [19,42].
2. The first approach to identify the main sources of reservoir sediments, which focused on the study of REE, was based on the comparison of the content, spatial distribution, and fractionation patterns of REE in sediments with those of representative soils and rocks from their catchments. In this study, only the REE data of sediments and soils were presented and discussed, since the geochemistry of rocks has already been analyzed and presented in [25,26]. In the case of soils, the variability of REE distribution testifies to the inheritance from a mixture of different lithotypes scattered in the catchments and the inclusion of particles originated from rocks in rugged areas that are, therefore, more easily eroded. Different conditions such as climate, relief, vegetation, and organisms could promote different soil development and pedogenic processes and alter the distribution of REE in soils derived from similar lithological sources. Changes in the content and distribution of these elements could be due to changes in the content of clay, clay minerals, and other REE-bearing minerals, aluminum, iron, manganese, organic matter, carbonate, and pH values, with which REE are usually positively associated [52]. These processes, responsible for the REE migration from the soils and the possible mixing of lithotypes of different natures, exclude soils as good tracers for defining the origin of the sediments deposited in these Dominican reservoirs, based solely on their data. This definition requires data from other sources, so data on the distribution of REE in the rocks of the basins were used.
 3. The comparative study of the composition and geochemical behavior of REE in sediments, soils, and rocks provided an initial approach to the areas of greater influence on sedimentation of the two reservoirs. Although it was possible to trace the likely sources of sediment, it was not possible to distinguish influences for each area of the reservoirs because of the homogeneity of spatial and seasonal REE patterns. Although there is not a very consistent fingerprinting model, the source areas are consistent with those based on other geochemical tracers, namely major (SiO_2 , Al_2O_3 , TiO_2 , MgO , CaO , K_2O , Na_2O , and MnO) and trace (Ba, Sr, Ni, Cu, Co, Zn, Pb, and Cr) elements presented in previous studies [26,59–61].
 4. This was the first study to trace the sources of sediments deposited in these two Dominican reservoirs. To obtain a more accurate geochemical signature, data from the REE study will be compared to other fingerprinting techniques that incorporate other chemical tracers and statistical analyses to distinguish and quantify the contribution of sources and differences between regions in each reservoir.
 5. A robust model on sediments provenance will help identify the most vulnerable areas in the watersheds and the presence of intense human activities to assist appropriate management and remediation strategies in erosion hotspots. Excessive erosion of these soils in a climate of intense annual precipitation characterized by periodic extreme climatic events has greatly increased sedimentation rates in these systems. Excessive siltation of reservoirs has led to degradation of water quality and energy production, and loss of storage capacity, which is of great concern to the national authorities responsible for managing water resources.

Author Contributions: Conceptualization, R.F.; methodology, R.F., C.G.P. and J.F.A.; software, J.F.A.; validation, R.F. and J.F.A.; formal analysis, R.F., C.G.P. and J.F.A.; investigation, R.F., C.G.P. and J.F.A.; resources, R.F.; data curation, R.F.; writing—original draft preparation, R.F.; writing—R.F., and J.F.A.; visualization, R.F., C.G.P. and J.F.A.; supervision, R.F.; project administration, R.F.; funding acquisition, R.F. All authors have read and agreed to the published version of the manuscript.

Funding: Financial support provided by FONDOCyT (Ministerio de la Educación Superior, Ciencia y Tecnología de la República Dominicana—MESCyT) through the Project “Aprovechamiento de los sedimentos de los embalses como nutrientes para la fertilización de suelos agrícolas en la República Dominicana”. Some equipment was purchased under the Project INALENTEJO—QREN 2007-2013 (projects ALENT-07-0262-FEDER-001867, ALENT-07-02622-FEDER-001876).

Institutional Review Board Statement: Not applicable.

Informed Consent Statement: Not applicable.

Data Availability Statement: Not applicable.

Acknowledgments: The authors acknowledge the funding provided by ICT, under contract with FCT (the Portuguese Science and Technology Foundation) and by the European Regional Development Fund through COMPETE 2020—Programa Operacional Competitividade e Internacionalização (POCI).

Conflicts of Interest: The authors declare that they have no conflict of interest.

References

1. Wetzel, M.A.; Wahrenndorf, D.S.; von der Ohe, P.C. Sediment pollution in the Erbe estuary and its potential toxicity at different trophic levels. *Sci. Total Environ.* **2013**, *449*, 199–207. [[CrossRef](#)]
2. Ding, S.; Han, C.; Wang, Y.; Yao, L.; Wang, Y.; Xu, D.; Zhang, C. In situ, high-resolution imaging of labile phosphorus in sediments of a large eutrophic lake. *Water Res.* **2015**, *74*, 100–109. [[CrossRef](#)]
3. Pang, H.; Pan, B.; Garzanti, E.; Gao, H.; Zhao, X.; Chen, D. Mineralogy and geochemistry of modern Yellow River sediments: Implications for weathering and provenance. *Chem. Geol.* **2018**, *488*, 76–86. [[CrossRef](#)]
4. Shao, J.Q.; Yang, S.Y.; Li, C. Chemical indices (CIA and WIP) as proxies for integrated chemical weathering in China: Influence from analysis of fluvial sediments. *Sediment. Geol.* **2012**, *265–266*, 110–120. [[CrossRef](#)]
5. Garzanti, E.; Padoan, M.; Setti, M.; López-Galindo, A.; Villa, I.M. Provenance versus weathering control on the composition of tropical river mud (southern Africa). *Chem. Geol.* **2014**, *366*, 61–74. [[CrossRef](#)]
6. Garzanti, E.; Resentini, A. Provenance control on chemical indices of weathering (Taiwan river sands). *Sediment. Geol.* **2016**, *336*, 81–95. [[CrossRef](#)]
7. Taylor, S.R.; McLennan, S.M. Chemical Composition and Element Distribution in the Earth’s Crust. In *The Continental Crust: Its Composition and Evolution*; Taylor, S.R., McLennan, S.M., Eds.; Blackwell: Oxford, UK, 1985; pp. 697–719.
8. Schneider, S.; Hornung, J.; Hinderer, M.; Garzanti, E. Petrography and geochemistry of modern river sediments in an equatorial environment (Rwenzori Mountains and Albertine Rift, Uganda): Implications for weathering and provenance. *Sediment. Geol.* **2016**, *336*, 106–119. [[CrossRef](#)]
9. Rollinson, H. *Using Geochemical Data: Evaluation, Presentation, Interpretation*; Pearson Education Ltd.: London, UK, 1993; p. 380.
10. Moermond, C.T.A.; Tijink, J.; Wetzel, A.P.V.; Koelmans, A.A. Distribution, speciation, and bioavailability of lanthanides in the Rhine-Meuse Estuary, The Netherlands. *Environ. Toxicol. Chem.* **2001**, *20*, 1916–1926. [[CrossRef](#)]
11. Wang, L.; Han, X.; Liang, T.; Guo, Q.; Li, J.; Dai, L.; Ding, S. Discrimination of rare earth element geochemistry and co-occurrence in sediment from Poyang Lake, the larger freshwater lake in China. *Chemosphere* **2019**, *217*, 851–857. [[CrossRef](#)]
12. Jones, A.P.; Wall, F.; Williams, C.T. *Rare Earth Minerals: Chemistry, Origin and Ore Deposits*; Chapman and Hall: London, UK, 1996; p. 372. ISBN 0412610302.
13. Wang, L.; Han, X.; Ding, S.; Liang, T.; Zhang, Y.; Xiao, J.; Dong, L.; Zhang, H. Combining multiple methods for provenance discrimination based on rare earth element geochemistry in lake sediment. *Sci. Total Environ.* **2019**, *672*, 264–274. [[CrossRef](#)]
14. Singh, P. Major, trace and REE geochemistry of the Ganga River sediments: Influence of provenance and sedimentary processes. *Chem. Geol.* **2009**, *266*, 242–255. [[CrossRef](#)]
15. Aide, M.; Aide, C. Rare Earth Elements: Their Importance in Understanding Soils Genesis. *Int. Sch. Res. Netw.* **2012**, *783876*, 11. [[CrossRef](#)]
16. Khan, A.M.; Abu Bakar, N.K.; Abu Bakar, A.F.; Ashraf, M.A. Chemical speciation and bioavailability of rare earth elements (REEs) in the ecosystem: A review. *Environ. Sci. Pollut.* **2017**, *24*, 22764–22789. [[CrossRef](#)] [[PubMed](#)]
17. Gwenzhi, W.; Mangori, L.; Danha, C.; Chaukura, N.; Dunjana, N.; Sanganyado, E. Sources, behaviour and environmental and human health risks of high-technology rare earth elements as emerging contaminants. *Sci. Total Environ.* **2018**, *636*, 299–313. [[CrossRef](#)] [[PubMed](#)]
18. Nozaki, Y. Rare earth elements and their isotopes in the ocean. In *Encyclopedia of Ocean Sciences*; Steele, J.H., Thorpe, S.A., Turekian, K.K., Eds.; Academic Press: San Diego, CA, USA, 2003; pp. 2354–2366.

19. Caetano, M.; Vale, C.; Anes, B.; Raimundo, J.; Drago, T.; Schmidt, S.; Nogueira, M.; Oliveira, A.; Prego, R. The Condor seamount at Mid-Atlantic Ridge as a supplementary source of trace and rare earth elements to the sediments. *Deep Sea Res.* **2013**, *PTII 98*, 24–37. [[CrossRef](#)]
20. Li, L.; Su, J.; Rao, W.; Wang, Y. Using geochemistry of rare earth elements to indicate sediment provenance of sand ridges in Southwestern Yellow Sea. *Chin. Geogr. Sci.* **2017**, *27*, 63–77. [[CrossRef](#)]
21. Laveuf, C.; Cornu, S. A review on the potentiality of rare earth elements to trace pedogenetic processes. *Geoderma* **2009**, *154*, 1–12. [[CrossRef](#)]
22. Chen, K.; Yang, C.; Jiao, J.J. Rare earth elements geochemistry and provenance discrimination of sediments in Tolo Harbour, Hong Kong. *Mar. Georesour. Geotec.* **2013**, *33*, 51–57. [[CrossRef](#)]
23. Infraeco. *Relevamientos Batimétricos y Estudios de Calidad del Agua y Sedimentación: Proyecto de Recuperación de Emergência y Gestión del Riesgo por Desastres Naturales*; Componente 1. Préstamo BIRF 7546-DO; Producto n° 2. Informe de Diagnóstico; Instituto Nacional de Recursos Hidráulicos (INDRHI): Santo Domingo, Dominican Republic, 2015; p. 284.
24. Fonseca, R.; Araújo, J.; Pinho, C.; Nogueira, P.; Araújo, A. Geochemistry of Rare Earth Elements (REE) as a Fingerprint of Sediment Provenance in Dominican Dam Reservoirs. In *XII Congresso Ibérico de Geoquímica: Extended Abstracts*, 1st ed.; Nogueira, P., Moreira, N., Roseiro, J., Maia, M., Eds.; Évora University: Evora, Portugal, 2019; pp. 57–60; ISBN 9789727781218.
25. Araújo, J. *Assinatura Geoquímica e Proveniência dos Sedimentos Depositados em Albufeiras Dominicanas*. Master's Thesis, University of Évora, Evora, Portugal, 2020; p. 218. (In Portuguese)
26. Fonseca, R.; Landa, B.; Pinho, C.; Araújo, J.; Nogueira, P.; Araújo, A. *Aprovechamiento de los Sedimentos de los Embalses como Nutrientes para la Fertilización de Suelos Agrícolas en la República Dominicana; Final Report and 8 Interim Reports of the Consortium Project between the University of Évora and the National Institute of Water Resources through the "Centro para la Gestión Sostenible de los Recursos Hídricos en los Estados Insulares del Caribe CEHICA (República Dominicana)"—FONDOCyT*; University of Évora: Evora, Portugal, 2019.
27. Pettijohn, E.J. *Sedimentary Rocks*, 3rd ed.; Harper & Row Publishers: New York, NY, USA, 1975; p. 628.
28. Pansu, M.; Gautheyrou, J. *Handbook of Soil Analysis: Mineralogical, Organic and Inorganic Methods*; Springer: Berlin/Heidelberg, Germany, 2006; p. 993; ISBN 9783540312116.
29. Zachmann, D.W. Matrix effects in the separation of rare-earth elements, scandium, and yttrium and their determination by inductively coupled plasma optical emission spectrometry. *Anal. Chem.* **1988**, *60*, 420–427. [[CrossRef](#)]
30. Watkins, P.J.; Nolan, J. Determination of rare-earth elements, yttrium, scandium and hafnium using cation-exchange separation and inductively coupled plasma-atomic emission spectrometry. *Chem. Geol.* **1992**, *95*, 131–139. [[CrossRef](#)]
31. Navarro, M.S.; Ulbrich, H.H.G.J.; Andrade, S.; Janasi, V.A. Adaptation of ICP-OES routine determination techniques for the analysis of rare earth elements by chromatographic separation in geological materials: Tests with reference materials and granitic rocks. *J. Alloys Compd.* **2002**, *344*, 40–45. [[CrossRef](#)]
32. White, W.M. *Geochemistry*; Wiley-Blackwell: Chichester, UK, 2013; p. 660. ISBN 978047065668.
33. Pedersen, T.L. Package 'ggforce': Accelerating 'ggplot2', version 0.3.3. MIT File Licence, Copyright Holder: Thomas Lin Pederson. 2021. Available online: <https://cran.r-project.org/> (accessed on 15 January 2021).
34. Meyer, M.A.; Booker, J.M. *Eliciting and Analysing Expert Judgment: A Practical Guide*; ASA-SIAM Series on Statistics and Applied Probability; Cambridge University Press: Cambridge, UK, 2001; p. 459; ISBN 0898714745.
35. Garthwaite, P.H.; Kadane, J.B.; O'Hagan, A. Statistical methods for eliciting probability distributions. *JASA* **2005**, *100*, 680–700. [[CrossRef](#)]
36. Phuong, N.; Truong, G.; Heuvelink, B.M.; Gosling, J.P. Web-based tool for expert elicitation of the variogram. *Comput. Geosci.* **2013**, *51*, 390–399.
37. Henderson, P. General geochemical properties and abundances of the rare earth elements. *Dev. Geochem.* **1984**, *2*, 1–32.
38. Vital, H.; Statterger, K.; Garbe-Schonberg, C.D. Composition and trace element geochemistry of detrital clay and heavy mineral suites of the lowermost Amazon River: A provenance study. *J. Sediment. Res.* **1999**, *69*, 563–575. [[CrossRef](#)]
39. Zhang, C.S.; Wang, L.J.; Li, G.S.; Dong, S.; Yang, J.; Wang, X. Grain size effect on multi-element concentration in sediments from the intertidal flats of Bohai Bay, China. *Appl. Geochem.* **2002**, *17*, 59–68. [[CrossRef](#)]
40. Cullers, R.L.; Basu, A.; Sutner, L.J. Geochemical signature of provenance in san-mixed material in soils and stream sediments near the Tobacco Root batholith, Montana, USA. *Chem. Geol.* **1988**, *70*, 335–348. [[CrossRef](#)]
41. Dinali, G.S.; Root, R.A.; Amistadi, M.K.; Chorover, J.; Lopes, G.; Guilherme, L.R.G. Rare earth elements (REY) sorption on soils of contrasting mineralogy and texture. *Environ. Int.* **2019**, *128*, 279–291. [[CrossRef](#)]
42. Alfaro, M.R.; Nascimento, C.W.A.; Biondi, C.M.; Bezzera da Silva, Y.; Bezzera da Silva, Y.; Accioly, A.M.; Montero, A.; Ugarte, O.M.; Estevez, J. Rare-earth-element geochemistry in soils developed in different geological settings of Cuba. *Catena* **2018**, *162*, 317–324. [[CrossRef](#)]
43. Yoshida, S.; Maramutsu, Y.; Tagami, K.; Uchida, S. Concentrations of lanthanide elements, Th, and U in 77 Japanese surface soils. *Environ. Int.* **1998**, *24*, 275–286. [[CrossRef](#)]
44. Tyler, G.; Olsson, T. Conditions related to solubility of rare and minor elements in forest soils. *J. Plant Nutr. Soil Sci.* **2002**, *165*, 594–601. [[CrossRef](#)]

45. Sadeghi, M.; Morris, G.A.; Carranza, E.J.M.; Ladenberger, A.; Andersson, M. Rare earth element distribution and mineralization in Sweden: An application of principal component analysis to FOREGS soil geochemistry. *J. Geochem. Explor.* **2013**, *133*, 160–175. [[CrossRef](#)]
46. Bezerra da Silva, Y.; Nascimento, C.W.A.; Bezerra da Silva, Y.; Biondi, C.M.; Cruz Silva, C. Rare earth element concentrations in Brazilian Benchmark soils. *Ver. Bras. Ciênc. Solo* **2016**, *40*. [[CrossRef](#)]
47. White, W.M.; Klein, E.M. Composition of the Oceanic Crust. In *Treatise on Geochemistry*, 2nd ed.; Turekian, K., Holland, H., Eds.; Elsevier Science: Amsterdam, The Netherlands, 2014; Volume 4, pp. 749–806. [[CrossRef](#)]
48. Jiménez-Reyes, M.; Solache-Ríos, M. Chemical behavior of lanthanum in the presence of soils componentes: Adsorption and humate complexes. *Water Air Soil Pollut.* **2014**, *225*, 1–13. [[CrossRef](#)]
49. Salminen, R. *Foregs, Geochemical Atlas of Europe*; EuroGeosurveys: Brussels, Belgium, 2005; ISBN 9516909132.
50. Kabata-Pendias, A.; Pendias, H. *Trace Elements in Soils and Plants*, 3rd ed.; CRC Press: Boca Raton, FL, USA, 2001; p. 403.
51. Mihajlovic, J.; Rinklebe, J. Rare earth elements in German soils—A review. *Chemosphere* **2018**, *205*, 514–523. [[CrossRef](#)]
52. Taylor, S.R.; McLennan, S.M. *Planetary Crusts: Their Composition, Origin and Evolution*; Cambridge University Press: Cambridge, UK, 2009; p. 402.
53. Erel, Y.; Stolper, E.M. Modelling of rare-earth element partitioning between particles and solution in aquatic environments. *Geochim. Cosmochim. Acta* **1993**, *57*, 513–518. [[CrossRef](#)]
54. Yang, S.Y.; Jung, H.S.; Choi, M.S.; Li, C.X. The rare earth element compositions of the Changjiang (Yangtze) and Huanghe (Yellow) river sediments. *Earth Planet Sci. Lett.* **2002**, *201*, 407–419. [[CrossRef](#)]
55. Prego, R.; Caetano, M.; Bernárdez, P.; Brito, P.; Ospina-Alvarez, N.; Vale, C. Rare earth elements in coastal sediments of the northern Galician shelf: Influence of geological features. *Cont. Shelf Res.* **2012**, *35*, 75–85. [[CrossRef](#)]
56. Liu, S.; Zhang, H.; Zhu, A.; Wang, K.; Chen, M.; Khokiattiwong, S.; Kornkanitnan, N.; Shi, X. Distribution of rare earth elements in surface sediments of the western Gulf of Thailand: Constraints from sedimentology and mineralogy. *Quat. Int.* **2019**, *527*, 52–63. [[CrossRef](#)]
57. Nath, B.N.; Roelandts, I.; Sudhakar, M.; Plüger, W. Rare earth element patterns of the Central Indian Basin sediments related to their lithology. *Geophys. Res. Lett.* **1992**, *19*, 1197–1200. [[CrossRef](#)]
58. Behrens, M.K.; Pahnke, K.; Paffrath, R.; Schnetger, B.; Brumsack, H.-J. Rare earth element distributions in the West Pacific: Trace element sources and conservative vs. non-conservative behavior. *Earth Planet Sci. Lett.* **2018**, *486*, 166–177. [[CrossRef](#)]
59. Araújo, J.; Nogueira, P.; Fonseca, R.; Pinho, C.; Araújo, A. Geochemistry of lacustrine sediments in systems with high sedimentation rates due to extreme climatic events: Case studies in the Dominican Republic; XCNG-17724. In Proceedings of the X Congresso Nacional de Geologia, Ponta Delgada, Portugal, 10–13 July 2018; Laboratório Nacional de Energia e Geologia: Amadora, Portugal, 2018; Volume II, pp. 45–48.
60. Araújo, J.; Albuquerque, T.; Fonseca, R.; Nogueira, P.; Pinho, C.; Araújo, A. Determination of spatial enrichment/impoverishment clusters in tropical soils—A Dominican Republic case study. In *XII Congresso Ibérico de Geoquímica: Extended Abstracts*, 1st ed.; Nogueira, P., Moreira, N., Roseiro, J., Maia, M., Eds.; Évora University: Évora, Portugal, 2019; pp. 57–60; ISBN 9789727781218.
61. Fonseca, R.; Pinho, C.; Araújo, J. Impact of extreme climatic events on the spatial and temporal distribution of major and trace elements in bed sediments of reservoir in the Dominican Republic; Geophysical Research Abstracts. In Proceedings of the 21st EGU General Assembly, Vienna, Austria, 7–12 April 2019; European Geosciences Union: Munich, Germany, 2019; Volume 21, p. EGU20195957.